axioms

MDPI

Article

Advanced Analysis of the Newly Unit-Lindley Model Under Improved Censoring: Applications to Biomedical and Engineering Systems

Heba S. Mohammed [1], Ahmed Elshahhat [2,*], Osama E. Abo-Kasem [3] and Asmaa Abdel-Hakim [4]

[1] Department of Mathematical Sciences, College of Science, Princess Nourah bint Abdulrahman University, P.O. Box 84428, Riyadh 11671, Saudi Arabia; hsmohammed@pnu.edu.sa
[2] Faculty of Technology and Development, Zagazig University, Zagazig 44519, Egypt
[3] Department of Statistics, Faculty of Commerce, Zagazig University, Zagazig 44519, Egypt
[4] Faculty of Management and International Economy, El Saleheya El Gadida University, New Salhia 44813, Egypt; a.hakim@sgu.edu.eg
* Correspondence: aelshahhat@ftd.zu.edu.eg

Abstract

In modern reliability and survival analysis, modeling bounded-lifetime data under complex sampling mechanisms remains a challenging yet practically significant problem, particularly in biomedical and engineering applications where experimental time and cost constraints are critical. This study develops a comprehensive inferential framework for the unit-Lindley (ULind) distribution under the improved adaptive progressive Type-II censoring (I-AP-CT2) strategy, a flexible design that ensures bounded test duration while accommodating progressive removal of experimental units. The proposed approach integrates both classical and Bayesian paradigms to enable robust estimation of the model parameter, reliability function, and hazard rate function. Maximum likelihood estimators are derived, and their asymptotic properties are established, with interval estimation constructed via normal approximation and log-transformed techniques. To address analytical intractability, a Bayesian framework via MCMC-based is formulated with a gamma prior, yielding credible and highest posterior density intervals. An extensive Monte Carlo simulation study is conducted to evaluate estimator performance under diverse censoring scenarios, demonstrating that Bayesian procedures consistently outperform their frequentist counterparts in terms of accuracy, stability, and interval efficiency. The practical relevance of the proposed methodology is illustrated through two real-world applications involving kidney dialysis survival data and petroleum engineering reliability data, representing critical domains where accurate modeling of failure behavior directly impacts clinical decision-making and industrial risk management. The findings highlight the flexibility of the ULind model in capturing complex hazard rate shapes and confirm the effectiveness of the I-AP-CT2 mechanism as a realistic and efficient experimental design.

Keywords: unit-Lindley; likelihood; Bayes MCMC-based; Markov iterative; Newton–Raphson; normality and log-normality intervals; improved censoring; model election; reliability; real data modelling

MSC: 62F10; 62F15; 62N01; 62N02; 62N05

Check for updates

Academic Editor: Hari Mohan Srivastava

Received: 7 April 2026
Revised: 24 April 2026
Accepted: 24 April 2026
Published: 27 April 2026

Copyright: © 2026 by the authors. Licensee MDPI, Basel, Switzerland. This article is an open access article distributed under the terms and conditions of the Creative Commons Attribution (CC BY) license.

1. Introduction

A new one-parameter bounded model, proposed by Mazucheli et al. [1], as an alternative to the standard Lindley distribution and referred to as the unit-Lindley (ULind(ϑ)) distribution, has emerged as an efficient and practically relevant framework for modeling data on the interval $(0, 1]$. This model combines parsimony with strong inferential capability, capturing diverse distributional shapes using a single parameter while retaining closed-form expressions for key functions such as the density, cumulative distribution, and moments, which greatly simplify estimation and simulation. In contrast to classical alternatives such as the Beta, Kumaraswamy, and Topp–Leone distributions, which often require two parameters and sometimes lack analytical tractability, the ULind model achieves comparable or superior goodness-of-fit with reduced computational complexity. Furthermore, its membership in the exponential family enables straightforward likelihood-based inference and supports regression modeling with covariates.

The failure rate of the ULind(ϑ) demonstrates remarkable flexibility and adaptability in modeling lifetime or reliability data on the unit interval $(0, 1)$. Unlike many classical bounded and unbounded distributions, whose HRFs are typically monotone (increasing or decreasing) or possess limited shapes, the HRF of this model can exhibit a wide range of behaviors, including bathtub-shaped, unimodal, and strictly increasing forms, depending on the parameter ϑ. This versatility allows the model to capture complex risk patterns in practical applications, such as early-life failures, wear-out periods, or mixed-risk scenarios, which are often encountered in clinical, engineering, and environmental studies. Such adaptable hazard behavior is largely unavailable in several existing distributions, providing a clear advantage for statistical modeling and reliability analysis where accurate representation of varying risk profiles is critical. Empirical evidence demonstrates its superiority through improved model selection criteria and better fit to real datasets, making it a robust and compelling alternative for analyzing proportion and rate data across diverse applied fields.

Let Y be a bounded lifetime random variable, symbolized by $Y \sim \text{ULind}(\vartheta)$ with $\vartheta > 0$ as the scale parameter, then its probability density function (PDF, $f(\cdot)$) and cumulative distribution function (CDF, $F(\cdot)$) are given by

$$f(y;\vartheta) = \frac{\vartheta^2}{(\vartheta+1)y^3} e^{-\vartheta y^\star}, \quad 0 < y < 1, \tag{1}$$

and

$$F(y;\vartheta) = \frac{(\vartheta+y)}{(\vartheta+1)y} e^{-\vartheta y^\star}, \tag{2}$$

respectively, where $y^\star = \frac{1-y}{y}$.

Assessing the reliability and failure rate functions provides critical information about a system's longevity and failure behavior. The reliability function reflects the likelihood that the system operates beyond a specified time, while the failure rate describes the instantaneous probability of failure. These functions play a key role in fields such as engineering, healthcare, and industrial applications. Accordingly, the reliability function (RF, $R(\cdot)$) and hazard (or failure) rate function (HRF, $h(\cdot)$) at time $0 < x < 1$, of the ULind lifespan model, are given by

$$R(x;\vartheta) = 1 - \frac{(\vartheta+x)}{(\vartheta+1)x} e^{-\vartheta x^\star}, \quad 0 < x < 1, \tag{3}$$

and

$$h(x;\vartheta) = \left(\frac{\vartheta}{x}\right)^2 \left[x(1+\vartheta)e^{\vartheta x^\star} - (x+\vartheta)\right]^{-1}, \tag{4}$$

https://doi.org/10.3390/axioms15050310

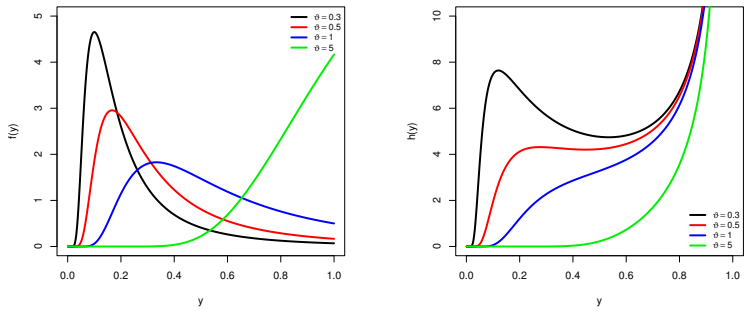
respectively, where $x^\star = \frac{1-x}{x}$; see Mazucheli et al. [1] for additional details.

Theorem 1. *The HRF of the ULind model, $h(x;\vartheta)$, exhibits flexible shapes depending on the parameter ϑ. Specifically, it provides*

- *A bathtub shape for small values of ϑ;*
- *A unimodal shape for moderate values of ϑ;*
- *A monotone increasing shape for large values of ϑ.*

Proof: See Appendix A.

Upon various choices of ϑ, Figure 1a reveals that the PDF (1) can be unimodal and right-skewed; for smaller parameter values, they exhibit a sharp peak followed by a monotone decreasing tail, while for larger values, the peak flattens and the distribution becomes more spread out. In contrast, Figure 1b exhibits that the HRF (4) provides diverse shapes, including bathtub-shaped forms, unimodal patterns, and strictly increasing behaviors, reflecting substantial flexibility in modeling early-life, mid-life, and wear-out failure mechanisms.



(**a**) PDF (**b**) HRF

Figure 1. Shapes of the ULind(ϑ) distribution.

In reliability and survival analysis, several censoring mechanisms have been proposed, generally categorized into one-stage and multi-stage procedures. One-stage censoring involves no unit removals during the experiment; the study continues uninterrupted until either a predetermined duration is reached or a specified number of failures occurs. Classical Type-I and Type-II censoring schemes belong to this category. In contrast, multi-stage designs provide greater flexibility by allowing units to be withdrawn at scheduled points before the experiment concludes. Notable examples include progressive Type-I and Type-II censoring (P-CT2), which have been extensively studied in the literature [2]. To reduce testing time and costs, Kundu and Joarder [3] introduced the hybrid progressive Type-I censoring scheme. Building on this idea, Ng et al. [4] proposed the adaptive progressive Type-II censoring (AP-CT2) framework, which generalizes the P-CT2 as a special case. This design permits early termination if the study duration exceeds a pre-specified limit and, as noted by Ng et al. [4], provides reliable statistical inference when the overall experiment time is not a primary concern.

However, for highly reliable units, AP-CT2 may result in excessively long experiments, which is impractical when test duration is critical. To address this, Yan et al. [5] developed the improved AP-CT2 (I-AP-CT2) scheme. This method offers two primary advantages: it guarantees the experiment concludes within a predefined time frame and encompasses several multi-stage censoring strategies, including both P-CT2 and AP-CT2 designs. Formally, consider n items placed on test with a target of k failures, a P-CT2 plan $\mathbf{S} = (S_1, \ldots, S_k)$, and two thresholds $t_{min} < t_{max}$. When the ith failure occurs at time $Y_{i:k:n}$, S_i remaining units are randomly withdrawn. Within this plan, three scenarios may arise:

- Scenario 1: If $Y_{k:k:n} < t_{min}$, the experiment ends at $Y_{k:k:n}$, corresponding to the standard P-CT2;
- Scenario 2: If $t_{min} < Y_{k:k:n} < t_{max}$, the experiment concludes at $Y_{k:k:n}$ after modifying the P-CT2 at $Y_{d_{min}:k:n}$ by setting $S_{d_{min}+1} = \cdots = S_{k-1} = 0$, where d_{min} is the number of failures observed before t_{min}. All remaining units are removed after the kth failure, corresponding to the AP-CT2;
- Scenario 3: If $t_{max} < Y_{k:k:n}$, the test stops at t_{max}. The P-CT2 is adapted by setting $S_{d_{min}+1} = \cdots = S_{d_{max}-1} = 0$, where $d_{max} < k$ is the number of failures observed before t_{max}. At t_{max}, all remaining units are withdrawn, with total $S^* = n - d_{max} - \sum_{i=1}^{d_{min}} S_i$.

Let $\mathbf{y} = \{(Y_1, S_1), \ldots, (Y_{d_{min}}, S_{d_{min}}), (Y_{d_{min}+1}, 0), \ldots, (Y_{d_{max}-1}, 0), (Y_{d_{max}}, S^\star)\}$ denote the I-AP-CT2 order statistics of size d_{max} drawn from a continuous population with PDF $f(\cdot)$ and RF $R(\cdot)$.

The corresponding joint likelihood function (JLF, $\mathcal{L}(\cdot)$) for this sample can then be expressed as:

$$\mathcal{L}(\vartheta \mid \mathbf{y}) \propto \prod_{i=1}^{\mathtt{C}_2} f(y_i; \vartheta) \prod_{i=1}^{\mathtt{C}_1} [R(y_i; \vartheta)]^{S_i} [R(t^\star; \vartheta)]^{S^\star}, \tag{5}$$

where $y_i \equiv Y_{i:k:n}$ for simplicity; see Table 1. For clarity, Figure 2 displays as a visual design of the I-AP-CT2 strategy.

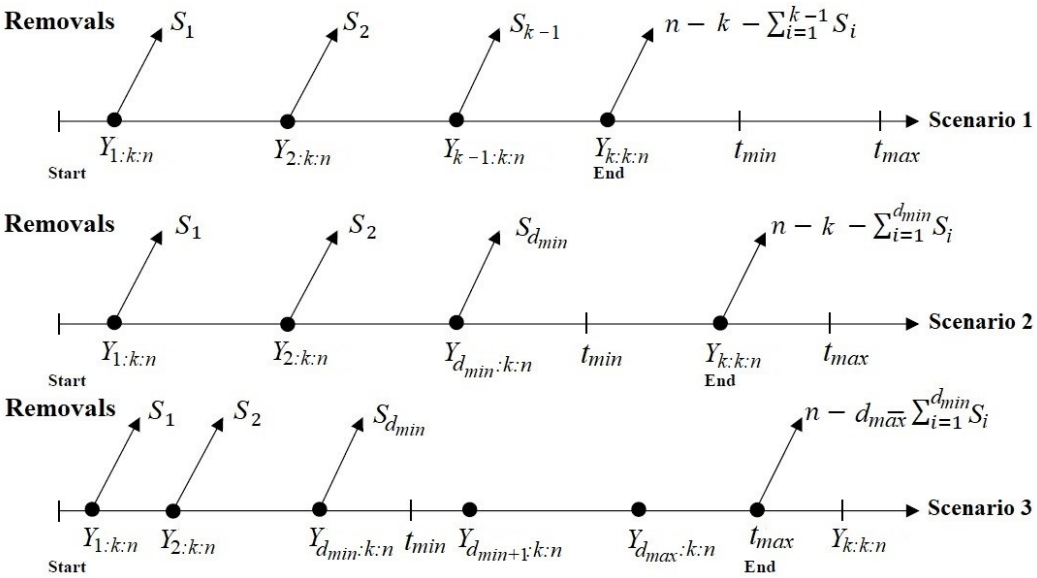


Figure 2. Visual design of the I-AP-CT2 plan.

Table 1. Options of $t^\star$, $S^\star$, and $\mathtt{C}_i$, $i = 1, 2$.

Scenario	$\mathtt{C}_1$	$\mathtt{C}_2$	$S^\star$	$t^\star$	$\{y_i, S_i\}$
1	$k-1$	k	S_k	y_k	$\{(y_1, S_1), \ldots, (y_{k-1}, S_{k-1}), (y_k, S^\star)\}$
2	d_{min}	k	$n - k - \sum_{i=1}^{d_{min}} S_i$	y_k	$\{(y_1, S_1), \ldots, (y_{d_{min}}, S_{d_{min}}), (y_{j_1+1}, 0), \ldots, (y_{k-1}, 0), (y_k, S^\star)\}$
3	d_{min}	d_{max}	$n - d_{max} - \sum_{i=1}^{d_{min}} S_i$	t_{max}	$\{(y_1, S_1), \ldots, (y_{d_{min}}, S_{d_{min}}), (y_{d_{min}+1}, 0), \ldots, (y_{d_{max}-1}, 0), (y_{d_{max}}, 0)\}$

Several commonly used censoring schemes arise as special cases of the I-AP-CT2 framework in Equation (5). Specifically, the T1-HPC scheme of Kundu and Joarder [3] is obtained by setting $t = t_{min} = t_{max}$. When $t_{max} \to \infty$, the model reduces to the AP-CT2 scheme introduced by Ng et al. [4]. Likewise, letting $t_{min} \to \infty$ yields the P-CT2 scheme of Balakrishnan and Cramer [2]. Finally, the T2-C scheme of Bain and Engelhardt [6] is recovered by taking $t_{min} \to 0$ together with $S_i = 0$ for $i = 1, 2, \ldots, k-1$ and $S_k = n - k$.

In this framework, the lower time level t_{min} serves as an initial alert level indicating that the experiment has entered a critical phase, whereas the upper time level t_{max} determines the maximum allowable duration of the test. If the preassigned number of failures k is not observed before reaching t_{max}, the experiment is terminated at that point. This modification addresses a key limitation of the AP-CT2 scheme of Ng et al. [4], where the experiment could otherwise continue for an excessively long period. By imposing the constraint t_{max}, the total testing time is ensured to remain within a fixed and finite range. Owing to these advantages, the scheme has been widely adopted in inferential studies; see, for instance, Nassar and Elshahhat [7], Elshahhat et al. [8], Zhang and Yan [9], and Dey and Kayal [10], among others.

The analysis of lifetime and reliability data in modern applications often involves bounded observations subject to complex censoring mechanisms, particularly in biomedical and engineering contexts where experimental constraints are unavoidable. While the ULind distribution offers a flexible and parsimonious framework for modeling data on the unit interval, its inferential performance under advanced censoring schemes has not been adequately explored. In many real-world studies, such as kidney dialysis survival analysis and petroleum engineering reliability assessments, data are collected under time restrictions and progressive withdrawal of experimental units, making classical censoring approaches insufficient. The I-AP-CT2 addresses these challenges by ensuring a bounded experimental duration while preserving inferential efficiency. Motivated by the need for robust statistical tools capable of handling such realistic data structures, this study develops a unified inferential framework for the ULind model under the I-AP-CT2 scheme, with direct applicability to clinically and industrially relevant datasets.

The inferential procedures developed in this study constitute a unified framework for analyzing the ULind model under the I-AP-CT2 censoring scheme. In the first stage, frequentist methods based on maximum likelihood estimation are developed to obtain point and interval estimates of the model parameter ϑ, RF $R(x)$, and HRF $h(x)$. In the second stage, a Bayesian framework is constructed for the same quantities using MCMC-based sampling and credible intervals. The simulation study and real-data applications are then used to compare the frequentist and Bayesian procedures in terms of estimation accuracy, interval efficiency, and coverage performance. Therefore, together the two parts provide a comprehensive inferential assessment of the proposed censored ULind model. The key novel contributions of this work can be summarized as follows:

- Maximum likelihood (ML) estimators for ϑ, $R(x)$, and $h(x)$ are derived, along with asymptotic intervals based on both normal approximation and log-transformation techniques.
- A full Bayesian framework is established using gamma prior, with posterior inference implemented via Markov chain Monte Carlo (MCMC) methods, enabling the construction of two credible interval types.
- Employ Newton–Raphson optimization for likelihood analysis and the Metropolis–Hastings algorithm for posterior sampling, ensuring computational feasibility despite model complexity.
- A large-scale simulation analysis evaluates estimator performance under various censoring configurations using multiple accuracy metrics, providing strong empirical validation.
- The proposed methodology is applied to kidney dialysis survival data, which are crucial for understanding patient survival patterns, treatment effectiveness, and risk dynamics in medical decision-making, and to petroleum engineering reliability data, which are essential for assessing system durability, failure behavior, and maintenance planning in industrial operations. These applications highlight the model's ability

to capture diverse failure mechanisms and provide reliable inference in high-stakes real-world settings.

The remainder of the paper is organized as follows. Sections 2 and 3 present the frequentist and Bayesian procedures, respectively. Monte Carlo simulations, along with their discussion, are provided in Section 4. In Section 5, two practical applications are illustrated. Finally, concluding remarks and key observations are summarized in Section 6.

2. Maximum Likelihood Inference

This section focuses on ML estimation for obtaining both point and interval estimates of the parameters ϑ, $R(x)$, and $h(x)$. To proceed, let $\{\mathbf{y}\}$ denote an I-AP-CT2 sample drawn from the proposed ULind distribution.

2.1. Point Estimators

The aim here is to derive the corresponding MLEs of ϑ, $R(x)$, and $h(x)$, denoted by $\widehat{\vartheta}$, $\widehat{R}(x)$, and $\widehat{h}(x)$, respectively. By utilizing expressions (1), (2), and (5), the JLF (5) can be rewritten as:

$$\mathcal{L}(\vartheta|\mathbf{y}) \propto \vartheta^{2\mathtt{C}_2}(\vartheta+1)^{-\mathtt{C}_2} e^{-\vartheta\sum_{i=1}^{\mathtt{C}_2} y_i^\star} \prod_{i=1}^{\mathtt{C}_1} [1-\Xi(y_i;\vartheta)]^{S_i} [1-\Xi(t^\star;\vartheta)]^{S^\star}, \tag{6}$$

where $\Xi(y_i;\vartheta) = \frac{(\vartheta+y_i)}{(\vartheta+1)y_i} e^{-\vartheta y_i^\star}$.

The corresponding log-JLF of (6) becomes

$$\begin{aligned}\log \mathcal{L}(\vartheta|\mathbf{y}) \propto\ & 2\mathtt{C}_2 \log(\vartheta) - \mathtt{C}_2 \log(\vartheta+1) - \vartheta \textstyle\sum_{i=1}^{\mathtt{C}_2} y_i^\star \\ & + \textstyle\sum_{i=1}^{\mathtt{C}_1} S_i \log[1-\Xi(y_i;\vartheta)] + S^\star \log[1-\Xi(t^\star;\vartheta)].\end{aligned} \tag{7}$$

Thus, the MLE $\widehat{\vartheta}$ of ϑ is given by:

$$\begin{aligned}\widehat{\wp}(\widehat{\vartheta}) =\ & \frac{\mathtt{C}_2(\vartheta+2)}{\vartheta(\vartheta+1)} - \textstyle\sum_{i=1}^{\mathtt{C}_2} y_i^\star \\ & - \textstyle\sum_{i=1}^{\mathtt{C}_1} S_i \Xi^\bullet(y_i;\vartheta)[1-\Xi(y_i;\vartheta)]^{-1} - S^\star \Xi^\bullet(t^\star;\vartheta)[1-\Xi(t^\star;\vartheta)]\Big|_{(\vartheta=\widehat{\vartheta})} = 0,\end{aligned} \tag{8}$$

where $\Xi^\bullet(y_i;\vartheta) = \frac{\vartheta^2}{(\vartheta+1)y_i^3} e^{-\vartheta y_i^\star}$.

Computationally, the MLE $\widehat{\vartheta}$ is obtained by solving the nonlinear likelihood form in (8). To accomplish this, the Newton–Raphson (NR) iterative method via installing the maxLik package version 4.2.2 (by Henningsen and Toomet [11]) is utilized. Let $\eth(\vartheta)$ represent the score function corresponding to (8), and let $\eth^\circ(\vartheta)$ denote its derivative with respect to ϑ. Beginning with an initial value $\vartheta^{(0)} > 0$, the iterative procedure is updated as follows:

$$\vartheta^{[j+1]} = \vartheta^{[j]} - \frac{\eth(\vartheta^{[j]})}{\eth^\circ(\vartheta^{[j]})}, \qquad j = 0,1,2,\ldots, \tag{9}$$

and continues until convergence is attained. The stopping rule is based on either a sufficiently small relative difference between successive iterates (for instance, less than 10^{-8}) or a near-zero value of the score function. This procedure provides a reliable and computationally efficient means of estimating ϑ.

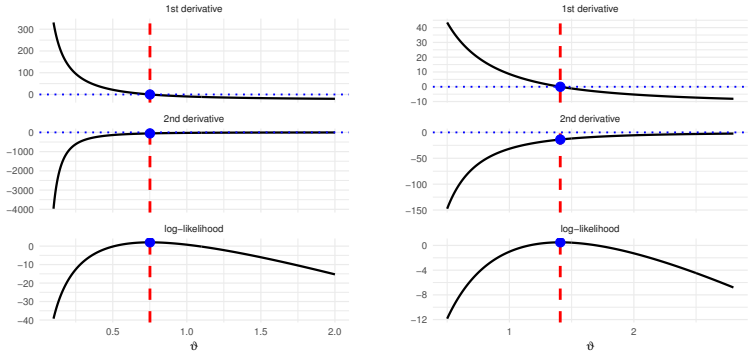
It is essential to examine the existence and uniqueness of the MLE $\widehat{\vartheta}$. Due to the intricate form of the score equation in (8), deriving these properties analytically is challenging. To address this issue, a numerical investigation is conducted based on samples generated

from the I-AP-CT2 scheme under the ULind distribution. Two different parameter settings are considered, namely $\vartheta \in \{0.8,\ 1.5\}$, with the experimental configuration $n = 50$, $k = 25$, $(t_{min}, t_{max}) = (1, 2)$, and $S_i = 1,\ i = 1, 2, \ldots, k$. The corresponding MLE values of ϑ from $\vartheta \in \{0.8,\ 1.5\}$ are obtained as $\widehat{\vartheta} \in \{0.7511,\ 1.4085\}$. Figure 3 presents the log-JLF along with its first and second derivatives. It can be observed that the vertical line corresponding to the MLE coincides with the peak of the estimated log-JLF and intersects the score function at zero. These graphical findings provide strong numerical evidence supporting the existence and uniqueness of the MLE of ϑ.

Furthermore, the invariance property of the MLE $\widehat{\vartheta}$ can be easily invoked to derive the corresponding estimates of the RF $R(x)$ and HRF $h(x)$. Accordingly, the MLEs $\widehat{R}(x)$ and $\widehat{h}(x)$ for $0 < x < 1$ are obtained directly as follows:

$$\widehat{R}(x;\widehat{\vartheta}) = 1 - \frac{(\widehat{\vartheta}+x)}{(\widehat{\vartheta}+1)x} e^{-\widehat{\vartheta}x^{\star}} \quad \text{and} \quad \widehat{h}(x;\widehat{\vartheta}) = \left(\frac{\widehat{\vartheta}}{x}\right)^{2} \left[x(1+\widehat{\vartheta})e^{\widehat{\vartheta}x^{\star}} - (x+\widehat{\vartheta})\right]^{-1},$$

respectively.



(**a**) $\vartheta = 0.8$ (**b**) $\vartheta = 1.5$

Figure 3. The existence and uniqueness diagram of ϑ.

2.2. Asymptotic Interval Estimators

In this subsection, in addition to the point estimation issues, constructing $100(1-\varrho)\%$ asymptotic confidence intervals (ACIs) for the parameters ϑ, $R(x)$, and $h(x)$ is of primary importance. These intervals rely on the large-sample behavior of the MLE $\widehat{\vartheta}$, which is asymptotically normally distributed with mean ϑ and covariance–variance (CV) matrix $\mathsf{V}(\cdot)$. Although the theoretical CV matrix is defined via the Fisher information (FI) matrix, denoted by $\mathsf{I}(\cdot)$, its explicit form is generally difficult to obtain for the model under consideration. To circumvent this issue, the CV matrix is approximated using the inverse of the observed Fisher information (FI) matrix evaluated at the MLE, namely $\mathsf{I}^{-1}(\cdot)\big|_{\vartheta=\widehat{\vartheta}}$. Subsequently, the estimated CV matrix can be formulated as:

$$\mathsf{V}(\widehat{\vartheta}) = \left[\mathsf{C}_2\left[\frac{\vartheta^2+4\vartheta+2}{\vartheta^2(\vartheta+1)^2}\right] + \sum_{i=1}^{\mathsf{C}_1} S_i\psi(y_i;\vartheta) + S^{\star}\psi(t^{\star};\vartheta)\right]^{-1}_{(\widehat{\vartheta}=\vartheta)}, \tag{10}$$

with

$$\psi(y_i;\vartheta) = [1-\Xi(y_i;\vartheta)]^{-1}\left\{\Xi^{\bullet\bullet}(y_i;\vartheta) - \Xi^{\bullet}(y_i;\vartheta)[1-\Xi(y_i;\vartheta)]^{-1}\right\}$$

where $\Xi^{\bullet\bullet}(y_i;\vartheta) = \Xi^{\bullet}(y_i;\vartheta)\left[\frac{(\vartheta+2)}{\vartheta(\vartheta+1)} - y_i^{\star}\right]$.

For the construction of $100(1-\varrho)\%$ ACIs associated with the RF $R(x)$ and HRF $h(x)$, it is necessary to approximate the variances of their estimators, $\widehat{R}(x)$ and $\widehat{h}(x)$. This can be effectively achieved using the delta method, yielding variance estimators denoted by

$\widehat{\mathsf{V}}_{\widehat{R}}$ and $\widehat{\mathsf{V}}_{\widehat{h}}$. Following Greene [12], the delta method implies that $\widehat{R}(x)$ is approximately normally distributed with mean $R(x)$ and variance $\widehat{\mathsf{V}}_{\widehat{R}}$, while $\widehat{h}(x)$ is approximately normal with mean $h(x)$ and variance $\widehat{\mathsf{V}}_{\widehat{h}}$; see Lawless [13]. Consequently, the expressions for $\widehat{\mathsf{V}}_{\widehat{R}}$ and $\widehat{\mathsf{V}}_{\widehat{h}}$ are given by:

$$\widehat{\mathsf{V}}_{\widehat{R}} = \mathsf{V}(\vartheta)\Lambda_R^2\Big|_{\vartheta=\widehat{\vartheta}} \quad \text{and} \quad \widehat{\mathsf{V}}_{\widehat{h}} = \mathsf{V}(\vartheta)\Lambda_h^2\Big|_{\vartheta=\widehat{\vartheta}},$$

respectively, with

$$\Lambda_R = -\Xi^{\bullet}(x^{\star};\vartheta)$$

and

$$\Lambda_h = \frac{2\vartheta\mathcal{A} - \vartheta^2\mathcal{A}^{\star}}{x^2A^2},$$

where $\mathcal{A} = x(1+\vartheta)e^{\vartheta x^{\star}} - (x+\vartheta)$ and $\mathcal{A}^{\star} = e^{\vartheta x^{\star}}\left[x + (1-x)(1+\vartheta)\right] - 1$.

Consequently, the $(1-\varrho)100\%$ ACI based on the normal approximation (say, NA-ACI) of ϑ, $R(x)$, and $h(x)$ (at a significance level $\varrho\%$) are given, respectively, by

$$\widehat{\vartheta} \mp z_{0.5\varrho}\sqrt{\mathsf{V}(\widehat{\vartheta})}, \quad \widehat{R}(x) \mp z_{0.5\varrho}\sqrt{\widehat{\mathsf{V}}_{\widehat{R}}}, \quad \text{and} \quad \widehat{h}(x) \mp z_{0.5\varrho}\sqrt{\widehat{\mathsf{V}}_{\widehat{h}}}$$

where $z_{0.5\varrho}$ is the upper 0.5ϱth standard Gaussian percentile point.

A notable limitation of the conventional NA-ACI approach is that it may yield lower confidence limits that are negative, even when the parameter of interest is inherently positive. In applied settings, such negative bounds are often truncated to zero; however, this adjustment is arbitrary and lacks a rigorous statistical justification. To address this issue and improve the reliability of interval estimation, Meeker and Escobar [14] introduced the normality log-transformed (NT) approximation, commonly referred to as NT-ACI. Accordingly, the $(1-\varrho)100\%$ NT-ACI for the scale parameter ϑ can be expressed as

$$\log\left(\widehat{\vartheta}\right) \mp z_{0.5\varrho}\sqrt{\mathsf{V}(\log(\widehat{\vartheta}))},$$

is equivalent to

$$\widehat{\vartheta}\exp\left(\mp\frac{z_{0.5\varrho}}{\widehat{\vartheta}}\sqrt{\mathsf{V}(\widehat{\vartheta})}\right).$$

In a similar manner, the $(1-\varrho)100\%$ NT-ACI for $\widehat{R}(x)$ and $\widehat{h}(x)$ can be readily obtained. For computing the NA-ACI and NT-ACI interval estimators for $\widehat{\vartheta}$, $\widehat{R}(x)$, and $\widehat{h}(x)$, the NR algorithm is re-recommended here. This iterative procedure can be efficiently implemented using the maxLik package within the R statistical environment.

3. Bayesian Inference

This section develops Bayesian point and credible interval estimators for the ULind model parameters ϑ, $R(x)$, and $h(x)$. The Bayesian framework necessitates the specification of prior distributions as well as a loss function, both of which play a crucial role in shaping the resulting inference. However, selecting an appropriate prior for an unknown parameter is often nontrivial. As noted by Gelman et al. [15], there is no universally prescribed guideline for prior selection in Bayesian analysis. Since the parameter ϑ in the ULind model is restricted to positive values, the gamma distribution provides a natural and commonly used prior choice. Accordingly, we assume $\vartheta \sim \text{Gamma}(a,b)$, $a,b>0$, with the following prior density

$$\Upsilon(\vartheta) = \frac{b^a}{\Gamma(a)}\vartheta^{a-1}e^{-b\vartheta}, \ \vartheta > 0. \tag{11}$$

From (6) and (11), the posterior PDF (say $\mho(\cdot)$) of ϑ is

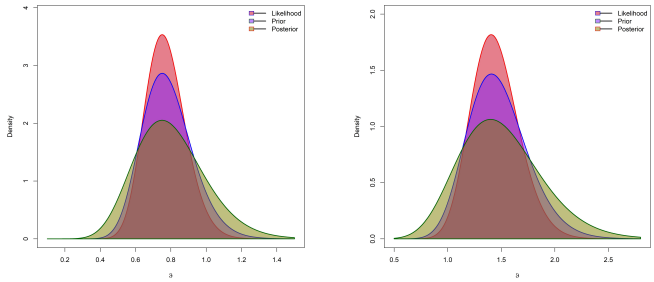
$$\mho(\vartheta|\mathbf{y}) \propto \vartheta^{2\mathtt{C}_2+a-1}(\vartheta+1)^{-\mathtt{C}_2} e^{-\vartheta\left(b+\sum_{i=1}^{\mathtt{C}_2}\right)y_i^\star} \prod_{i=1}^{\mathtt{C}_1}[1-\Xi(y_i;\vartheta)]^{S_i}[1-\Xi(t^\star;\vartheta)]^{S^\star}, \tag{12}$$

where its normalized term (say, Ψ) is given by $\Psi = \int_0^\infty \Upsilon(\vartheta) \times \mathcal{L}(\vartheta|\mathbf{y})\mathrm{d}\vartheta$.

Hence, to develop the Bayes estimator of ϑ, denoted by $\tilde{\vartheta}$, the squared-error loss (SEL) function is employed, as it is one of the most widely used symmetric loss functions in Bayesian estimation. It is worth noting, however, that the proposed methodology can be extended to incorporate alternative loss functions without fundamentally altering the estimation procedure. From (12) and (6), the Bayes estimator of ϑ, denoted by $\tilde{\vartheta}$, under the SEL is expressed as:

$$\begin{aligned} \tilde{\vartheta} &= \Psi^{-1}\int_0^\infty \vartheta^{2\mathtt{C}_2+a}(\vartheta+1)^{-\mathtt{C}_2} e^{-\vartheta\left(b+\sum_{i=1}^{\mathtt{C}_2}\right)y_i^\star} \\ &\times \prod_{i=1}^{\mathtt{C}_1}[1-\Xi(y_i;\vartheta)]^{S_i}[1-\Xi(t^\star;\vartheta)]^{S^\star}\mathrm{d}\vartheta. \end{aligned} \tag{13}$$

It can be observed from (13) that closed-form expressions for the Bayes estimators of ϑ, $R(x)$, and $h(x)$ are not attainable. To overcome this analytical intractability, an MCMC approach is employed to generate samples from the posterior distribution in (12). These simulated samples facilitate the computation of Bayesian mean estimate, as well as Bayes credible interval (BCI) and highest posterior density (HPD) interval for each parameters of interest. Although the posterior distribution of ϑ does not correspond to any standard continuous distribution, it exhibits a shape that is approximately normal, as depicted in Figure 4. Accordingly, the Metropolis–Hastings (M–H) algorithm is utilized to update the posterior samples of ϑ (see Algorithm 1). The generated posterior draws are subsequently used to obtain the Bayes estimates of ϑ, $R(x)$, and $h(x)$, along with their associated measures of uncertainty.



(**a**) $\vartheta = 0.8$ (**b**) $\vartheta = 1.5$

Figure 4. The likelihood, prior, and posterior density shapes of ϑ.

Algorithm 1 Estimating ϑ, $R(x)$, and $h(x)$ by MCMC Steps

1: **Input:** Initial value $\widehat{\vartheta}$, estimated variance $\widehat{\mathrm{V}}(\widehat{\vartheta})$, total number of iterations ∇, burn-in size ∇°, confidence level $(1-\varrho)$
2: **Output:** Posterior mean $\tilde{\vartheta}$, BCI and HPD intervals for ϑ
3: Initialize $\vartheta^{[0]} \leftarrow \widehat{\vartheta}$
4: Set $j \leftarrow 1$
5: **while** $j \leq \nabla$ **do**
6: Generate a candidate value $\vartheta^{\star} \sim N\big(\vartheta^{[j-1]}, \widehat{\mathrm{V}}(\widehat{\vartheta})\big)$
7: Compute the acceptance probability:

$$\aleph = \min\left\{1, \frac{\mho(\vartheta^{\star} \mid \mathbf{y})}{\mho(\vartheta^{[j-1]} \mid \mathbf{y})}\right\}$$

8: Draw $u \sim U(0,1)$
9: **if** $u \leq \aleph$ **then**
10: Set $\vartheta^{[j]} \leftarrow \vartheta^{\star}$
11: **else**
12: Set $\vartheta^{[j]} \leftarrow \vartheta^{[j-1]}$
13: **end if**
14: Update $R(x)$ from (3) and $h(x)$ from (4) using $\vartheta^{[j]}$
15: Set $j \leftarrow j+1$
16: **end while**
17: Discard the first ∇° samples as burn-in
18: Define $\nabla^{\bullet} = \nabla - \nabla^{\circ}$
19: Compute the posterior mean:

$$\tilde{\vartheta} = \frac{1}{\nabla^{\bullet}} \sum_{j=\nabla^{\circ}+1}^{\nabla} \vartheta^{[j]}$$

20: Sort the retained samples $\vartheta^{[j]}$, $j = \nabla^{\circ}+1, \ldots, \nabla$, in ascending order
21: Construct the $(1-\varrho)100\%$ BCI of ϑ as:

$$\left(\vartheta_{(0.5\varrho\nabla^{\bullet})},\ \vartheta_{((1-0.5\varrho)\nabla^{\bullet})}\right)$$

22: Construct the $(1-\varrho)100\%$ HPD of ϑ as:

$$\left(\vartheta_{[j^{\circ}]},\ \vartheta_{[j^{\circ}+(1-\varrho)\nabla^{\bullet}]}\right)$$

where j° minimizes:

$$\vartheta_{[j+(1-\varrho)\nabla^{\bullet}]} - \vartheta_{[j]}, \quad j = 1, \ldots, \varrho\nabla^{\bullet}$$

23: Repeat Steps 19–22 for $R(x)$ and $h(x)$

4. Monte Carlo Evaluations

To assess the estimation accuracy and empirical performance of the proposed estimators for ϑ, $R(x)$, and $h(x)$, an extensive Monte Carlo simulation study was conducted. Following Algorithm 2, the I-AP-CT2 was implemented 2000 times for each selected parameter configuration, specifically Pop-1:ULind($\vartheta = 0.5$) and Pop-2:ULind($\vartheta = 1.5$), to generate estimates of the target quantities. The associated reliability characteristics were computed as $(R(x), h(x)) = (0.99626, 0.26644)$ from Pop-1 at $x = 0.1$ and $(0.99157, 0.28122)$ from Pop-2 at $x = 0.2$. To further investigate the robustness of the estimation procedures, additional simulations were performed under a range of experimental settings determined by the threshold values t_{min} and t_{max}, the full sample size n, the observed number of failures k, and the censoring configuration **S**. In particular, the thresholds were selected as $t_{min} \in \{0.2, 0.5\}$ and $t_{max} \in \{0.5, 0.8\}$, while the sample sizes considered were

$n \in \{20, 50, 80\}$. Table 2 presents, for each value of n, the corresponding effective sample sizes k together with their associated P-CT2 censoring **S**.

Algorithm 2 Generation of an I-AP-CT2 Sample

Input: Sample size n, effective failures k, threshold times t_{min}, t_{max}, and censoring scheme **S**.
Specify the true parameter value of the ULindϑ distribution.
Generate k independent random variables $q_1, q_2, \ldots, q_k \sim U(0,1)$.
for $i = 1$ to k **do**
  Compute

$$b_i = q_i^{\left(i+\sum_{j=k-i+1}^{k} S_j\right)^{-1}}.$$

end for
for $i = 1$ to k **do**
  Compute

$$U_i = 1 - \prod_{j=k-i+1}^{k} b_j.$$

end for
for $i = 1$ to k **do**
  Obtain $y_i = G^{-1}(U_i; \vartheta)$.
end for
Record d_{min} observed failures at time t_{min}.
Remove y_i for $i = d_{min} + 2, \ldots, k$.
Define the truncated sample size as

$$n_{\text{trunc}} = n - d_{min} - 1 - \sum_{i=1}^{d_{min}} S_i.$$

Generate $y_{d_{min}+2}, \ldots, y_k$ from the truncated distribution with PDF $\frac{g(y)}{R(y_{d_{min}+1})}$
if $y_k < t_{min} < t_{max}$ **then**
  Case 1: Terminate the experiment at time y_k.
else if $t_{min} < y_k < t_{max}$ **then**
  Case 2: Terminate the experiment at time y_k.
else if $t_{min} < t_{max} < y_k$ **then**
  Case 3: Terminate the experiment at time t_{max}.
end if

Table 2. Different P-CT2 designs, **S**, in Monte Carlo simulations.

Design	(n,k)	Design	(n,k)
	(20, 10)		(20, 15)
A[11]	$(2^5, 0^5)$	A[21]	$(1^5, 0^{10})$
B[12]	$(0^2, 2^5, 0^3)$	B[22]	$(0^5, 1^5, 0^5)$
C[13]	$(0^5, 2^5)$	C[23]	$(0^{10}, 1^5)$
	(50, 20)		(50, 40)
A[11]	$(3^{10}, 0^{10})$	A[21]	$(1^{10}, 0^{30})$
B[12]	$(0^5, 3^{10}, 0^5)$	B[22]	$(0^{15}, 1^{10}, 0^{15})$
C[13]	$(0^{10}, 3^{10})$	C[23]	$(0^{30}, 1^{10})$
	(80, 30)		(80, 60)
A1[1]	$(5^{10}, 0^{20})$	A2[1]	$(1^{20}, 0^{40})$
B1[2]	$(0^{10}, 5^{10}, 0^{10})$	B2[2]	$(0^{20}, 1^{20}, 0^{20})$
C1[3]	$(0^{20}, 5^{10})$	C2[3]	$(0^{40}, 1^{20})$

For notational convenience, an expression such as 1^5 denotes that the individual experimental unit is removed at each of the first five censoring stages. Upon the 2000 generated I-AP-CT2 samples, point estimates and their corresponding 95% ACIs—namely,

the NA-ACI and NT-ACI—for ϑ, $R(x)$, and $h(x)$ were computed using the maxLik package (by Henningsen and Toomet [11]) within the R software environment (version 4.2.2).

For the Bayesian framework, a total of $\nabla = 12{,}000$ MCMC samples were generated, with the beginning $\nabla^{\circ} = 2{,}000$ iterations discarded as burn-in to ensure convergence. Posterior summaries, including point estimates and the corresponding 95% BCI and HPD interval results for ϑ, $R(x)$, and $h(x)$, were obtained using the coda package [16] within the same R computing environment.

To examine the robustness of the Bayesian estimation procedures, two alternative sets of hyperparameters, denoted by (a, b), were considered. In accordance with the prior specification approach of Kundu [17], the gamma prior parameters (a, b) were chosen as follows:

- Prior-A[PA] = $(4.0, 5)$ and Prior-B[PB] = $(8, 10)$ for $\vartheta = 0.8$;
- Prior-A[PA] = $(7.5, 5)$ and Prior-B[PB] = $(15, 10)$ for $\vartheta = 1.5$.

These hyperparameter selections were made such that the implied prior means align with reasonable values of ϑ. It is worth noting that PA reflects a relatively diffuse prior distribution with higher variance, representing limited prior knowledge, whereas PB corresponds to a more informative prior with reduced dispersion, guided by empirical insights into the scale behavior of the ULind model. The simulation results indicate that, although both prior specifications yield comparable posterior mean estimates, the use of PB leads to reduced posterior variability, shorter HPD intervals, and improved coverage probabilities. This demonstrates the beneficial effect of incorporating informative prior information without inducing noticeable bias.

To quantitatively evaluate the performance of the estimation results for ϑ, $R(x)$, or $h(x)$, the following summary measures are considered:

- Mean Point Estimate: $\mathrm{MPE}(\widehat{\vartheta}) = \frac{1}{2{,}000}\sum_{i=1}^{2{,}000}\widehat{\vartheta}^{[i]}$;
- Root Mean Squared Error: $\mathrm{RMSE}(\widehat{\vartheta}) = \sqrt{\frac{1}{2{,}000}\sum_{i=1}^{2{,}000}\left(\widehat{\vartheta}^{[i]} - \vartheta\right)^2}$;
- Average Relative Absolute Bias: $\mathrm{ARAB}(\widehat{\vartheta}) = \frac{1}{2{,}000}\sum_{i=1}^{2{,}000}\widehat{\vartheta}^{-1}\left|\widehat{\vartheta}^{[i]} - \vartheta\right|$;
- Average Interval Length: $\mathrm{AIL}_{95\%}(\vartheta) = \frac{1}{2{,}000}\sum_{i=1}^{2{,}000}\left(\mathsf{U}_{\widehat{\vartheta}^{[i]}} - \mathsf{L}_{\widehat{\vartheta}^{[i]}}\right)$;
- Coverage Probability: $\mathrm{CP}_{95\%}(\vartheta) = \frac{1}{2{,}000}\sum_{i=1}^{2{,}000}\Xi_{\left(\mathsf{L}_{\widehat{\vartheta}^{[i]}}, \mathsf{U}_{\widehat{\vartheta}^{[i]}}\right)}(\vartheta)$,

  where $\widehat{\vartheta}^{[i]}$ denotes the ith estimate of ϑ and $\Xi(\cdot)$ is the indicator function. The same precision metrics are also applied to the estimates of $R(x)$ and $h(x)$.

From the results presented in Tables 3–8, several important observations can be highlighted, with particular emphasis on configurations yielding lower RMSEs, ARABs, and AILs, along with higher CPs:

- Overall, the estimators of ϑ, $R(x)$, and $h(x)$ demonstrate satisfactory performance across all considered simulation settings.
- Estimation precision improves with increasing n (or equivalently), and similar improvements are observed when $\sum_{i=1}^{k} S_i$ decreases.
- Higher levels of t_{min} and t_{max} for $i = 1, 2$, for Pop-i ($i = 1, 2$), lead to enhanced estimation accuracy. In particular, RMSEs, ARABs, and AILs tend to decrease, whereas CPs show noticeable improvement.
- As the ULindϑ increases:
  - The RMSE and ARAB results of ϑ developed by the frequentist approach exhibit an increasing trend, while those developed by the MCMC iterative procedure narrow down.
  - The RMSE and ARAB results of $R(x)$ and $h(x)$ developed by the ML and MCMC iterative procedures decreased;

  - AILs expand for all quantities, accompanied by a slight reduction in CPs.
- Bayesian estimation based on MCMC sampling, along with the associated credible intervals, provides more stable and reliable results compared to frequentist methods, primarily due to the incorporation of prior information.
- For all examined values of ϑ, the Bayesian estimator under PB consistently yields superior performance relative to competing approaches, attributable to its lower prior variance compared to the other. A similar advantage is observed for credible intervals (BCI and HPD) when compared with asymptotic intervals (NA-ACI and NT-ACI).
- A comparative evaluation of the proposed censoring designs (A$[ij]$, B$[ij]$, and C$[ij]$) for $i = 1, 2$ and $j = 1, 2, 3$, in Table 2, for each combination of n and k, indicates that:
  - The most accurate estimation of ϑ is achieved using C$[i3]$ for ($i = 1, 2$), corresponding to right censoring;
  - The estimation of $h(x)$ is most precise using B$[i2]$ for ($i = 1, 2$), representing middle censoring;
  - The estimation of $R(x)$ is optimized using A$[i1]$ for ($i = 1, 2$), associated with left censoring.
- Comparing the proposed credible and asymptotic interval estimation methods:
  - The NA-ACI approach performs better than NT-ACI for ϑ and $h(x)$, whereas NT-ACI is more appropriate for $R(x)$;
  - All HPD intervals consistently outperform standard BCIs;
  - In general, both BCI and HPD approaches exhibit clear superiority over their asymptotic counterparts (NA-ACI and NT-ACI).
- In summary, from a practical reliability perspective, the ULind lifetime model is most effectively analyzed within a Bayesian framework, particularly when employing MCMC iterative techniques.

Table 3. The MPE (1st Col.), RMSE (2nd Col.), and ARAB (3rd Col.) results of ϑ.

$n(k)$	Design	MLE			Bayesian						MLE			Bayesian					
					PA			PB						PA			PB		
					$(t_{min}, t_{max}) = (0.2, 0.5)$									$(t_{min}, t_{max}) = (0.5, 0.8)$					
Pop-1																			
20(10)	A[11]	0.8279	0.3961	0.2780	0.8295	0.1623	0.1491	0.7935	0.1170	0.1144	0.6053	0.3196	0.2281	0.8111	0.1542	0.1435	0.7644	0.1148	0.0972
	B[12]	0.7841	0.4054	0.2841	0.8261	0.1748	0.1537	0.7846	0.1287	0.1239	0.5890	0.3282	0.2515	0.8127	0.1649	0.1476	0.7681	0.1259	0.1111
	C[13]	0.8559	0.3869	0.2672	0.8329	0.1615	0.1455	0.7963	0.1090	0.1042	0.6239	0.3134	0.2175	0.8117	0.1538	0.1407	0.7650	0.1055	0.0952
20(15)	A[21]	0.6646	0.3718	0.2496	0.8114	0.1362	0.1134	0.8273	0.1028	0.0952	0.5200	0.3085	0.2109	0.8005	0.1289	0.1044	0.8115	0.0997	0.0877
	B[22]	0.6573	0.3858	0.2570	0.8099	0.1402	0.1203	0.8260	0.1044	0.0968	0.5032	0.3130	0.2143	0.7993	0.1339	0.1114	0.8106	0.0997	0.0905
	C[23]	0.6278	0.3705	0.2337	0.8086	0.1309	0.1006	0.8245	0.0972	0.0864	0.5222	0.2995	0.2074	0.8018	0.1227	0.0973	0.8131	0.0917	0.0848
50(20)	A[11]	0.8756	0.3518	0.2138	0.8317	0.1043	0.0846	0.8737	0.0770	0.0640	0.6287	0.2900	0.1940	0.7842	0.1002	0.0792	0.8284	0.0735	0.0568
	B[12]	0.7974	0.3568	0.2206	0.8173	0.1072	0.0872	0.8615	0.0816	0.0782	0.6104	0.2939	0.1947	0.7879	0.1023	0.0839	0.8296	0.0812	0.0744
	C[13]	0.9638	0.3476	0.2030	0.8377	0.1040	0.0835	0.8822	0.0754	0.0609	0.6421	0.2881	0.1861	0.7853	0.0999	0.0791	0.8296	0.0722	0.0546
50(40)	A[21]	0.6135	0.2520	0.1802	0.7111	0.0820	0.0707	0.7872	0.0591	0.0552	0.4914	0.2224	0.1659	0.7009	0.0791	0.0655	0.7713	0.0567	0.0536
	B[22]	0.6009	0.2698	0.1971	0.7096	0.0830	0.0796	0.7872	0.0600	0.0562	0.4757	0.2348	0.1683	0.6931	0.0801	0.0718	0.7702	0.0568	0.0536
	C[23]	0.5777	0.2468	0.1685	0.7061	0.0812	0.0666	0.7803	0.0591	0.0535	0.4904	0.2116	0.1640	0.7007	0.0787	0.0629	0.7713	0.0551	0.0533
80(30)	A[11]	0.9135	0.2354	0.1598	0.7887	0.0612	0.0554	0.8917	0.0518	0.0502	0.6297	0.2030	0.1569	0.7266	0.0602	0.0528	0.8234	0.0510	0.0480
	B[12]	0.7525	0.2375	0.1637	0.7429	0.0613	0.0561	0.8386	0.0528	0.0516	0.6026	0.2055	0.1575	0.7250	0.0605	0.0529	0.8256	0.0517	0.0492
	C[13]	1.0269	0.2159	0.1518	0.7992	0.0601	0.0552	0.9027	0.0511	0.0490	0.6420	0.1869	0.1500	0.7263	0.0584	0.0517	0.8230	0.0493	0.0478
80(60)	A[21]	0.6376	0.2011	0.1331	0.7261	0.0570	0.0459	0.7548	0.0407	0.0372	0.5036	0.1770	0.1323	0.6984	0.0568	0.0452	0.7193	0.0407	0.0337
	B[22]	0.5946	0.2131	0.1459	0.7131	0.0583	0.0548	0.7443	0.0486	0.0418	0.4832	0.1786	0.1438	0.6948	0.0578	0.0502	0.7112	0.0470	0.0415
	C[23]	0.5862	0.1992	0.1275	0.7091	0.0551	0.0437	0.7392	0.0405	0.0346	0.5145	0.1690	0.1241	0.7010	0.0541	0.0435	0.7311	0.0405	0.0335
Pop-2																			
20(10)	A[11]	1.5738	0.5588	0.2725	1.5330	0.1417	0.0851	1.4948	0.0727	0.0513	1.3599	0.3684	0.1550	1.5291	0.1096	0.0781	1.4883	0.0583	0.0467
	B[12]	1.5772	0.5656	0.3396	1.5330	0.1434	0.0950	1.4945	0.0734	0.0583	1.2734	0.3725	0.2112	1.5261	0.1096	0.0813	1.4828	0.0597	0.0509
	C[13]	1.5261	0.5572	0.2643	1.5327	0.1381	0.0819	1.4927	0.0711	0.0508	1.3888	0.3640	0.1508	1.5292	0.1061	0.0751	1.4894	0.0566	0.0465
20(15)	A[21]	1.3896	0.5006	0.2592	1.5168	0.0997	0.0703	1.5334	0.0583	0.0412	1.1030	0.3188	0.1443	1.5057	0.0781	0.0595	1.5235	0.0479	0.0357
	B[22]	1.4365	0.5322	0.2618	1.5165	0.1035	0.0721	1.5322	0.0604	0.0413	1.4426	0.3515	0.1451	1.5111	0.0800	0.0608	1.5271	0.0484	0.0357
	C[23]	1.3786	0.4951	0.2490	1.5168	0.0900	0.0684	1.5334	0.0536	0.0394	1.3319	0.3138	0.1413	1.5054	0.0777	0.0595	1.5198	0.0467	0.0346
50(20)	A[11]	1.6717	0.4381	0.2334	1.5228	0.0654	0.0569	1.5688	0.0371	0.0338	1.4173	0.2864	0.1365	1.5119	0.0652	0.0554	1.5594	0.0349	0.0308
	B[12]	1.7214	0.4885	0.2381	1.5255	0.0899	0.0570	1.5735	0.0450	0.0343	1.2759	0.3091	0.1387	1.5068	0.0660	0.0554	1.5541	0.0377	0.0308
	C[13]	1.6210	0.4378	0.2287	1.5189	0.0639	0.0568	1.5672	0.0363	0.0331	1.5187	0.2688	0.1324	1.5201	0.0607	0.0541	1.5672	0.0348	0.0302
50(40)	A[21]	1.2966	0.3472	0.2130	1.4399	0.0616	0.0554	1.5177	0.0351	0.0330	1.4218	0.2135	0.1202	1.4200	0.0569	0.0469	1.5029	0.0343	0.0267
	B[22]	1.3645	0.3749	0.2131	1.4419	0.0624	0.0558	1.5180	0.0355	0.0330	1.5540	0.2196	0.1319	1.4177	0.0591	0.0469	1.4984	0.0348	0.0267
	C[23]	1.2922	0.3455	0.1939	1.4399	0.0584	0.0554	1.5177	0.0342	0.0323	1.4412	0.2119	0.1080	1.4183	0.0567	0.0459	1.5005	0.0329	0.0251
80(30)	A[11]	1.7246	0.2845	0.1496	1.4677	0.0537	0.0467	1.5767	0.0320	0.0259	1.4132	0.2059	0.1047	1.4610	0.0521	0.0456	1.5695	0.0291	0.0247
	B[12]	1.8136	0.3110	0.1785	1.4783	0.0551	0.0491	1.5893	0.0321	0.0274	1.1919	0.2060	0.1056	1.4397	0.0542	0.0457	1.5463	0.0314	0.0249
	C[13]	1.6506	0.2668	0.1469	1.4629	0.0536	0.0447	1.5724	0.0314	0.0246	1.5877	0.2002	0.0949	1.4677	0.0492	0.0446	1.5761	0.0290	0.0245
80(60)	A[21]	1.3032	0.2273	0.1245	1.4513	0.0527	0.0442	1.4823	0.0298	0.0236	1.5704	0.1839	0.0919	1.4240	0.0488	0.0410	1.4578	0.0289	0.0235
	B[22]	1.4030	0.2514	0.1404	1.4619	0.0535	0.0444	1.4943	0.0298	0.0237	1.5474	0.1847	0.0942	1.4171	0.0488	0.0411	1.4500	0.0290	0.0236
	C[23]	1.2970	0.1863	0.0987	1.4513	0.0514	0.0438	1.4823	0.0295	0.0235	1.4728	0.1434	0.0792	1.4140	0.0449	0.0410	1.4480	0.0264	0.0234

Table 4. The MPE (first col.), RMSE (second col.), and ARAB (third col.) results of $R(x)$.

$n(k)$	Design	MLE			Bayesian						MLE			Bayesian					
					PA			PB						PA			PB		
					$(t_{min}, t_{max}) = (0.2, 0.5)$									$(t_{min}, t_{max}) = (0.5, 0.8)$					
Pop-1																			
20(10)	A[11]	0.9958	0.5262	0.4873	0.9970	0.2285	0.1945	0.9958	0.1671	0.1285	0.9768	0.1115	0.0884	0.9961	0.0681	0.0455	0.9948	0.0405	0.0317
	B[12]	0.9937	0.5758	0.4992	0.9969	0.2324	0.1962	0.9958	0.1698	0.1370	0.9741	0.1128	0.0933	0.9961	0.0757	0.0566	0.9947	0.0475	0.0352
	C[13]	0.9907	0.5859	0.5446	0.9967	0.2437	0.2206	0.9955	0.2049	0.1477	0.9710	0.1344	0.0998	0.9962	0.0886	0.0655	0.9949	0.0502	0.0368
20(15)	A[21]	0.9799	0.5090	0.4299	0.9962	0.2093	0.1569	0.9968	0.0843	0.0655	0.9550	0.0565	0.0477	0.9959	0.0423	0.0378	0.9965	0.0304	0.0244
	B[22]	0.9846	0.5129	0.4757	0.9963	0.2174	0.1653	0.9969	0.0942	0.0716	0.9535	0.0626	0.0591	0.9958	0.0490	0.0423	0.9964	0.0390	0.0281
	C[23]	0.9813	0.5240	0.4823	0.9962	0.2216	0.1910	0.9968	0.1036	0.0771	0.9477	0.0696	0.0626	0.9957	0.0556	0.0432	0.9964	0.0404	0.0292
50(20)	A[11]	0.9985	0.3980	0.3782	0.9971	0.1377	0.1176	0.9980	0.0699	0.0483	0.9831	0.0224	0.0193	0.9946	0.0183	0.0180	0.9969	0.0179	0.0148
	B[12]	0.9966	0.4440	0.4144	0.9969	0.1680	0.1189	0.9979	0.0701	0.0485	0.9815	0.0235	0.0202	0.9945	0.0197	0.0190	0.9968	0.0183	0.0158
	C[13]	0.9935	0.4957	0.4198	0.9964	0.1775	0.1537	0.9977	0.0746	0.0509	0.9787	0.0437	0.0339	0.9947	0.0241	0.0215	0.9969	0.0209	0.0187
50(40)	A[21]	0.9743	0.2687	0.1980	0.9869	0.0830	0.0515	0.9942	0.0449	0.0287	0.9489	0.0205	0.0178	0.9856	0.0168	0.0156	0.9934	0.0136	0.0136
	B[22]	0.9806	0.2976	0.2236	0.9881	0.0937	0.0552	0.9948	0.0461	0.0294	0.9482	0.0215	0.0180	0.9858	0.0176	0.0174	0.9934	0.0149	0.0141
	C[23]	0.9773	0.3343	0.2544	0.9876	0.1296	0.0756	0.9947	0.0474	0.0300	0.9420	0.0218	0.0182	0.9835	0.0180	0.0177	0.9931	0.0169	0.0144
80(30)	A[11]	0.9992	0.1813	0.1482	0.9961	0.0405	0.0297	0.9983	0.0248	0.0170	0.9844	0.0153	0.0135	0.9916	0.0130	0.0130	0.9963	0.0125	0.0105
	B[12]	0.9979	0.2005	0.1766	0.9958	0.0498	0.0305	0.9982	0.0252	0.0172	0.9830	0.0161	0.0143	0.9916	0.0134	0.0131	0.9963	0.0131	0.0107
	C[13]	0.9918	0.2136	0.1771	0.9931	0.0754	0.0454	0.9971	0.0260	0.0176	0.9786	0.0174	0.0148	0.9914	0.0136	0.0135	0.9964	0.0133	0.0107
80(60)	A[21]	0.9767	0.1375	0.1192	0.9909	0.0284	0.0248	0.9929	0.0226	0.0160	0.9586	0.0122	0.0112	0.9899	0.0111	0.0106	0.9923	0.0094	0.0090
	B[22]	0.9846	0.1506	0.1327	0.9926	0.0288	0.0256	0.9941	0.0233	0.0164	0.9544	0.0124	0.0117	0.9893	0.0113	0.0108	0.9910	0.0102	0.0094
	C[23]	0.9769	0.1659	0.1328	0.9915	0.0304	0.0291	0.9934	0.0246	0.0169	0.9465	0.0128	0.0127	0.9888	0.0114	0.0113	0.9901	0.0111	0.0096
Pop-2																			
20(10)	A[11]	0.9905	0.6415	0.6151	0.9925	0.1420	0.1099	0.9912	0.0671	0.0489	0.9803	0.0456	0.0349	0.9923	0.0229	0.0221	0.9911	0.0211	0.0208
	B[12]	0.9922	0.6668	0.6206	0.9925	0.1423	0.1168	0.9913	0.0698	0.0506	0.9753	0.0478	0.0364	0.9923	0.0260	0.0226	0.9911	0.0221	0.0213
	C[13]	0.9918	0.6702	0.6349	0.9925	0.1517	0.1206	0.9913	0.0712	0.0514	0.9681	0.0478	0.0364	0.9922	0.0277	0.0251	0.9909	0.0242	0.0233
20(15)	A[21]	0.9823	0.5660	0.4882	0.9920	0.1214	0.1019	0.9925	0.0383	0.0316	0.9432	0.0220	0.0215	0.9916	0.0211	0.0194	0.9921	0.0189	0.0184
	B[22]	0.9831	0.5700	0.5129	0.9920	0.1324	0.1032	0.9925	0.0411	0.0354	0.9539	0.0220	0.0220	0.9916	0.0211	0.0199	0.9922	0.0196	0.0194
	C[23]	0.9851	0.6342	0.5475	0.9920	0.1380	0.1078	0.9924	0.0433	0.0370	0.9409	0.0231	0.0221	0.9918	0.0215	0.0202	0.9923	0.0196	0.0195
50(20)	A[11]	0.9941	0.3852	0.3629	0.9920	0.0710	0.0569	0.9934	0.0213	0.0205	0.9888	0.0179	0.0175	0.9920	0.0175	0.0161	0.9934	0.0157	0.0134
	B[12]	0.9952	0.4792	0.3819	0.9921	0.1017	0.0782	0.9934	0.0253	0.0210	0.9832	0.0196	0.0193	0.9917	0.0183	0.0162	0.9932	0.0157	0.0136
	C[13]	0.9958	0.4959	0.4597	0.9922	0.1167	0.0887	0.9935	0.0359	0.0277	0.9742	0.0213	0.0211	0.9916	0.0186	0.0172	0.9931	0.0157	0.0136
50(40)	A[21]	0.9798	0.2691	0.1899	0.9888	0.0582	0.0464	0.9920	0.0185	0.0172	0.9286	0.0162	0.0161	0.9874	0.0154	0.0152	0.9913	0.0148	0.0125
	B[22]	0.9802	0.2943	0.2302	0.9888	0.0620	0.0478	0.9920	0.0197	0.0180	0.9460	0.0170	0.0168	0.9875	0.0160	0.0157	0.9914	0.0155	0.0125
	C[23]	0.9844	0.3709	0.2531	0.9889	0.0650	0.0534	0.9920	0.0211	0.0192	0.9300	0.0175	0.0174	0.9873	0.0172	0.0158	0.9912	0.0157	0.0125
80(30)	A[11]	0.9947	0.1621	0.1109	0.9901	0.0485	0.0399	0.9936	0.0169	0.0158	0.9926	0.0155	0.0147	0.9903	0.0141	0.0138	0.9937	0.0122	0.0121
	B[12]	0.9961	0.2277	0.1349	0.9903	0.0505	0.0434	0.9937	0.0177	0.0161	0.9839	0.0156	0.0148	0.9900	0.0148	0.0142	0.9935	0.0124	0.0122
	C[13]	0.9971	0.2499	0.1844	0.9907	0.0542	0.0443	0.9940	0.0182	0.0162	0.9690	0.0156	0.0149	0.9890	0.0148	0.0142	0.9928	0.0124	0.0123
80(60)	A[21]	0.9809	0.0555	0.0405	0.9898	0.0366	0.0322	0.9909	0.0160	0.0153	0.9373	0.0145	0.0137	0.9880	0.0133	0.0131	0.9896	0.0116	0.0112
	B[22]	0.9814	0.1081	0.0712	0.9898	0.0382	0.0347	0.9909	0.0162	0.0153	0.9556	0.0146	0.0137	0.9886	0.0136	0.0134	0.9900	0.0117	0.0116
	C[23]	0.9868	0.1411	0.1017	0.9902	0.0428	0.0386	0.9913	0.0164	0.0155	0.9306	0.0147	0.0142	0.9882	0.0141	0.0138	0.9897	0.0121	0.0121

Table 5. The MPE (first col.), RMSE (second col.), and ARAB (third col.) results of $h(x)$.

$n(k)$	Design	MLE			Bayesian						MLE			Bayesian					
					PA			PB						PA			PB		
					$(t_{min}, t_{max}) = (0.2, 0.5)$									$(t_{min}, t_{max}) = (0.5, 0.8)$					
Pop-1																			
20(10)	A[11]	0.5031	1.9108	1.6262	0.2338	1.6082	1.3872	0.3091	1.3492	1.1233	1.3206	1.0621	0.8704	0.2655	0.7418	0.6675	0.3443	0.4370	0.2601
	B[12]	0.2706	1.8252	1.5364	0.2213	1.4385	1.2070	0.2887	1.1573	0.9748	1.1052	0.8897	0.7383	0.2691	0.6481	0.5961	0.3515	0.3389	0.2168
	C[13]	0.3659	1.8731	1.5941	0.2274	1.5211	1.2854	0.2927	1.2416	1.0866	1.2076	0.9839	0.7473	0.2707	0.7142	0.6278	0.3531	0.3809	0.2514
20(15)	A[21]	0.8062	1.6787	1.4287	0.2612	1.3042	1.1045	0.2286	0.9729	0.9390	1.9233	0.8349	0.5842	0.2884	0.4604	0.3149	0.2544	0.3085	0.2080
	B[22]	1.0024	1.6129	1.3642	0.2679	1.2580	1.0049	0.2326	0.9212	0.8349	1.8782	0.7711	0.5104	0.2837	0.4192	0.2940	0.2518	0.2500	0.1666
	C[23]	0.9202	1.7104	1.4897	0.2647	1.3824	1.1428	0.2303	1.0827	0.9464	2.1025	0.8565	0.6045	0.2924	0.4977	0.3553	0.2560	0.3149	0.2152
50(20)	A[11]	0.3881	1.5121	1.2869	0.2537	1.1757	0.9694	0.1777	0.8098	0.6778	1.0656	0.5029	0.4163	0.3419	0.3704	0.2356	0.2270	0.1396	0.1386
	B[12]	0.1169	1.3942	1.1866	0.2111	0.9985	0.9273	0.1566	0.6240	0.4290	0.8841	0.3935	0.3504	0.3483	0.3243	0.1304	0.2278	0.1240	0.1073
	C[13]	0.2253	1.4026	1.2136	0.2227	1.0252	0.9318	0.1644	0.7306	0.4705	0.9517	0.4079	0.3525	0.3522	0.3518	0.1356	0.2303	0.1295	0.1087
50(40)	A[21]	1.0017	1.1583	0.9858	0.6478	0.8241	0.5936	0.3377	0.4192	0.3759	2.1327	0.3528	0.3121	0.7339	0.2388	0.1208	0.4045	0.1024	0.1006
	B[22]	1.2522	1.0924	0.9297	0.6902	0.7942	0.5824	0.3686	0.3993	0.3588	2.1210	0.3146	0.3080	0.7382	0.2334	0.1155	0.4045	0.1020	0.0930
	C[23]	1.1234	1.2580	1.0894	0.6648	0.8945	0.6040	0.3405	0.5809	0.4015	2.3253	0.3832	0.3182	0.8139	0.2447	0.1222	0.4158	0.1154	0.1047
80(30)	A[11]	0.4810	1.0104	0.9025	0.4330	0.7512	0.3736	0.2150	0.3576	0.3039	1.0809	0.2947	0.2484	0.5129	0.1424	0.1003	0.2489	0.0897	0.0847
	B[12]	0.0674	0.9514	0.8097	0.2751	0.6492	0.3678	0.1329	0.2891	0.2809	0.8418	0.2426	0.2211	0.5036	0.1367	0.0949	0.2563	0.0839	0.0815
	C[13]	0.1548	0.9522	0.8981	0.2952	0.6553	0.3702	0.1414	0.3010	0.2827	0.9024	0.2506	0.2475	0.5024	0.1388	0.0989	0.2545	0.0879	0.0838
80(60)	A[21]	0.8424	0.8286	0.7052	0.4653	0.5932	0.3565	0.3842	0.2487	0.2239	1.9503	0.2135	0.1848	0.6125	0.1298	0.0764	0.5355	0.0683	0.0683
	B[22]	1.1663	0.7643	0.6505	0.5460	0.5253	0.3446	0.4438	0.2442	0.2135	1.8176	0.1994	0.1775	0.5896	0.1258	0.0751	0.4761	0.0683	0.0655
	C[23]	1.1461	0.8793	0.7483	0.5193	0.6320	0.3625	0.4211	0.2628	0.2550	2.2000	0.2178	0.2064	0.6354	0.1354	0.0806	0.5758	0.0781	0.0693
Pop-2																			
20(10)	A[11]	0.2636	1.4137	1.2144	0.2561	0.9956	0.4463	0.2887	0.3324	0.3263	0.7384	0.2405	0.2147	0.2620	0.1724	0.1199	0.2988	0.0720	0.0709
	B[12]	0.3001	1.3641	1.1812	0.2564	0.9072	0.4270	0.2903	0.3161	0.3143	0.5096	0.2066	0.2042	0.2593	0.1635	0.1149	0.2931	0.0623	0.0619
	C[13]	0.2553	1.4051	1.2069	0.2561	0.9675	0.4403	0.2885	0.3263	0.3249	0.6010	0.2107	0.2091	0.2595	0.1695	0.1199	0.2940	0.0678	0.0638
20(15)	A[21]	0.4703	1.2099	1.0731	0.2696	0.8720	0.3203	0.2558	0.2906	0.1967	1.0170	0.1920	0.1823	0.2799	0.1048	0.0594	0.2633	0.0593	0.0577
	B[22]	0.4879	1.1735	1.0351	0.2696	0.8451	0.2886	0.2558	0.2845	0.1920	1.2002	0.1779	0.1700	0.2802	0.0969	0.0593	0.2664	0.0587	0.0577
	C[23]	0.4214	1.2523	1.1063	0.2699	0.9039	0.3341	0.2566	0.3134	0.1999	1.2172	0.1927	0.1823	0.2749	0.1099	0.0606	0.2605	0.0606	0.0602
50(20)	A[11]	0.1535	1.0894	0.9501	0.2628	0.7451	0.2743	0.2256	0.2497	0.1734	0.6497	0.1594	0.1326	0.2801	0.0924	0.0576	0.2392	0.0556	0.0437
	B[12]	0.2070	0.9865	0.7780	0.2688	0.6069	0.1771	0.2298	0.1719	0.1655	0.3317	0.1551	0.1303	0.2677	0.0558	0.0558	0.2298	0.0486	0.0428
	C[13]	0.1744	1.0036	0.8815	0.2654	0.6645	0.2368	0.2287	0.1809	0.1730	0.4581	0.1556	0.1326	0.2753	0.0656	0.0564	0.2352	0.0505	0.0437
50(40)	A[21]	0.5473	0.7526	0.5642	0.3510	0.4849	0.1599	0.2685	0.1594	0.1573	1.1782	0.1468	0.1196	0.3798	0.0526	0.0507	0.2836	0.0461	0.0419
	B[22]	0.5552	0.6842	0.5630	0.3510	0.4679	0.1550	0.2685	0.1532	0.1496	1.4508	0.1439	0.1187	0.3830	0.0491	0.0483	0.2861	0.0447	0.0418
	C[23]	0.4529	0.8345	0.6904	0.3480	0.4977	0.1706	0.2680	0.1660	0.1619	1.4212	0.1503	0.1196	0.3843	0.0556	0.0539	0.2882	0.0478	0.0419
80(30)	A[11]	0.1137	0.6252	0.5113	0.3028	0.4213	0.1495	0.2138	0.1439	0.1427	0.7665	0.1195	0.1182	0.3454	0.0483	0.0447	0.2454	0.0413	0.0389
	B[12]	0.1889	0.4907	0.4032	0.3186	0.3493	0.1416	0.2252	0.1376	0.1323	0.2425	0.1147	0.1143	0.3137	0.0455	0.0421	0.2226	0.0411	0.0376
	C[13]	0.1463	0.5845	0.4459	0.3137	0.4107	0.1446	0.2222	0.1436	0.1425	0.4486	0.1180	0.1148	0.3211	0.0481	0.0446	0.2273	0.0412	0.0389
80(60)	A[21]	0.5251	0.4036	0.3556	0.3284	0.2444	0.1397	0.2989	0.1313	0.1135	1.0225	0.1126	0.1120	0.3588	0.0445	0.0416	0.3226	0.0376	0.0369
	B[22]	0.5350	0.3911	0.3257	0.3284	0.1420	0.1380	0.2989	0.1296	0.1103	1.3247	0.1083	0.1059	0.3714	0.0441	0.0416	0.3336	0.0361	0.0359
	C[23]	0.3967	0.4474	0.3717	0.3181	0.3139	0.1412	0.2883	0.1313	0.1259	1.4238	0.1143	0.1140	0.3675	0.0449	0.0420	0.3312	0.0393	0.0376

Table 6. The AIL (first col.) and CP (second col.) estimation results of ϑ.

$n(k)$	Design	NA-ACI		NT-ACI		BCI				HPD			
						PA		PB		PA		PB	
For Pop-1 $((t_{min}, t_{max}) = (0.2, 0.5))$													
20(10)	A[11]	0.485	0.953	0.646	0.940	0.173	0.979	0.161	0.980	0.145	0.981	0.140	0.981
	B[12]	0.490	0.953	0.677	0.937	0.181	0.978	0.168	0.979	0.157	0.980	0.149	0.981
	C[13]	0.483	0.953	0.635	0.940	0.173	0.979	0.158	0.980	0.145	0.981	0.135	0.982
20(15)	A[21]	0.435	0.957	0.530	0.949	0.159	0.980	0.140	0.981	0.139	0.982	0.134	0.982
	B[22]	0.442	0.956	0.531	0.949	0.160	0.980	0.141	0.981	0.140	0.981	0.134	0.982
	C[23]	0.429	0.958	0.513	0.951	0.157	0.980	0.140	0.981	0.138	0.982	0.134	0.982
50(20)	A[11]	0.309	0.968	0.420	0.958	0.152	0.980	0.140	0.982	0.132	0.982	0.131	0.982
	B[12]	0.314	0.967	0.465	0.955	0.156	0.980	0.140	0.982	0.137	0.982	0.131	0.982
	C[13]	0.308	0.968	0.407	0.959	0.151	0.981	0.139	0.982	0.132	0.982	0.130	0.982
50(40)	A[21]	0.258	0.972	0.341	0.965	0.149	0.981	0.132	0.982	0.128	0.983	0.126	0.983
	B[22]	0.262	0.971	0.388	0.961	0.150	0.981	0.137	0.982	0.129	0.982	0.127	0.983
	C[23]	0.255	0.972	0.313	0.967	0.148	0.981	0.131	0.982	0.127	0.983	0.125	0.983
80(30)	A[11]	0.242	0.973	0.301	0.968	0.144	0.981	0.126	0.983	0.123	0.983	0.118	0.983
	B[12]	0.251	0.972	0.305	0.968	0.147	0.981	0.126	0.983	0.124	0.983	0.122	0.983
	C[13]	0.240	0.973	0.293	0.969	0.142	0.981	0.125	0.983	0.122	0.983	0.116	0.983
80(60)	A[21]	0.205	0.976	0.237	0.973	0.137	0.982	0.119	0.983	0.117	0.983	0.106	0.984
	B[22]	0.213	0.975	0.248	0.973	0.142	0.981	0.120	0.983	0.117	0.983	0.114	0.984
	C[23]	0.204	0.976	0.235	0.974	0.136	0.982	0.119	0.983	0.116	0.983	0.099	0.985
For Pop-1 $((t_{min}, t_{max}) = (0.5, 0.8))$													
20(10)	A[11]	0.472	0.954	0.631	0.941	0.166	0.979	0.155	0.980	0.145	0.981	0.133	0.982
	B[12]	0.478	0.953	0.660	0.938	0.174	0.979	0.161	0.980	0.157	0.980	0.141	0.981
	C[13]	0.471	0.954	0.619	0.942	0.165	0.979	0.152	0.981	0.144	0.981	0.132	0.982
20(15)	A[21]	0.423	0.958	0.516	0.950	0.157	0.980	0.140	0.982	0.138	0.982	0.131	0.982
	B[22]	0.430	0.957	0.517	0.950	0.158	0.980	0.140	0.981	0.138	0.982	0.132	0.982
	C[23]	0.417	0.959	0.499	0.952	0.155	0.980	0.139	0.982	0.137	0.982	0.131	0.982
50(20)	A[11]	0.306	0.968	0.416	0.959	0.150	0.981	0.137	0.982	0.131	0.982	0.129	0.982
	B[12]	0.311	0.967	0.460	0.955	0.154	0.980	0.138	0.982	0.137	0.982	0.129	0.982
	C[13]	0.305	0.968	0.403	0.960	0.149	0.981	0.137	0.982	0.131	0.982	0.127	0.983
50(40)	A[21]	0.255	0.972	0.339	0.965	0.148	0.981	0.130	0.982	0.126	0.983	0.123	0.983
	B[22]	0.259	0.972	0.386	0.961	0.148	0.981	0.135	0.982	0.129	0.982	0.126	0.983
	C[23]	0.252	0.972	0.311	0.967	0.145	0.981	0.129	0.982	0.125	0.983	0.121	0.983
80(30)	A[11]	0.241	0.973	0.298	0.968	0.141	0.981	0.124	0.983	0.119	0.983	0.116	0.983
	B[12]	0.249	0.972	0.302	0.968	0.144	0.981	0.124	0.983	0.123	0.983	0.118	0.983
	C[13]	0.239	0.973	0.290	0.969	0.140	0.981	0.123	0.983	0.118	0.983	0.114	0.984
80(60)	A[21]	0.204	0.976	0.236	0.974	0.136	0.982	0.117	0.983	0.116	0.983	0.104	0.984
	B[22]	0.212	0.976	0.246	0.973	0.140	0.982	0.119	0.983	0.117	0.983	0.112	0.984
	C[23]	0.202	0.976	0.234	0.974	0.135	0.982	0.117	0.983	0.115	0.984	0.098	0.985
For Pop-2 $((t_{min}, t_{max}) = (0.2, 0.5))$													
20(10)	A[11]	1.139	0.932	1.300	0.924	0.169	0.980	0.149	0.981	0.145	0.981	0.140	0.981
	B[12]	1.167	0.930	1.337	0.922	0.171	0.980	0.149	0.981	0.145	0.981	0.140	0.981
	C[13]	1.102	0.934	1.271	0.925	0.168	0.980	0.147	0.981	0.142	0.981	0.138	0.981
20(15)	A[21]	0.918	0.943	1.140	0.932	0.143	0.981	0.142	0.981	0.140	0.981	0.136	0.982
	B[22]	0.957	0.941	1.188	0.929	0.147	0.981	0.144	0.981	0.140	0.981	0.138	0.981
	C[23]	0.913	0.943	1.133	0.932	0.143	0.981	0.141	0.981	0.140	0.981	0.135	0.982
50(20)	A[11]	0.729	0.952	0.863	0.945	0.142	0.981	0.140	0.981	0.139	0.981	0.130	0.982
	B[12]	0.774	0.950	0.907	0.943	0.143	0.981	0.140	0.981	0.139	0.981	0.134	0.982
	C[13]	0.689	0.954	0.843	0.946	0.142	0.981	0.140	0.981	0.139	0.981	0.128	0.982
50(40)	A[21]	0.568	0.960	0.702	0.953	0.139	0.981	0.133	0.982	0.125	0.982	0.123	0.982
	B[22]	0.630	0.957	0.760	0.951	0.141	0.981	0.138	0.981	0.125	0.982	0.123	0.982
	C[23]	0.551	0.961	0.687	0.954	0.135	0.982	0.133	0.982	0.124	0.982	0.122	0.982
80(30)	A[11]	0.519	0.963	0.652	0.956	0.129	0.982	0.123	0.982	0.118	0.982	0.116	0.983
	B[12]	0.523	0.962	0.680	0.955	0.132	0.982	0.125	0.982	0.122	0.982	0.120	0.982
	C[13]	0.517	0.963	0.650	0.956	0.129	0.982	0.116	0.983	0.114	0.983	0.113	0.983
80(60)	A[21]	0.424	0.967	0.516	0.963	0.125	0.982	0.114	0.983	0.109	0.983	0.108	0.983
	B[22]	0.450	0.966	0.557	0.961	0.127	0.982	0.115	0.983	0.113	0.983	0.108	0.983
	C[23]	0.407	0.968	0.514	0.963	0.123	0.982	0.113	0.983	0.109	0.983	0.108	0.983
For Pop-2 $((t_{min}, t_{max}) = (0.5, 0.8))$													
20(10)	A[11]	1.108	0.933	1.265	0.926	0.161	0.980	0.148	0.981	0.141	0.981	0.139	0.981
	B[12]	1.135	0.932	1.299	0.924	0.163	0.980	0.148	0.981	0.141	0.981	0.139	0.981
	C[13]	1.070	0.935	1.236	0.927	0.161	0.980	0.147	0.981	0.138	0.981	0.137	0.981
20(15)	A[21]	0.890	0.944	1.110	0.933	0.143	0.981	0.141	0.981	0.137	0.981	0.135	0.982
	B[22]	0.929	0.942	1.157	0.931	0.146	0.981	0.142	0.981	0.138	0.981	0.137	0.981
	C[23]	0.886	0.944	1.103	0.934	0.141	0.981	0.141	0.981	0.137	0.982	0.134	0.982
50(20)	A[11]	0.721	0.953	0.854	0.946	0.141	0.981	0.140	0.981	0.135	0.982	0.129	0.982
	B[12]	0.765	0.950	0.897	0.944	0.141	0.981	0.140	0.981	0.136	0.982	0.132	0.982
	C[13]	0.681	0.955	0.834	0.947	0.141	0.981	0.139	0.981	0.135	0.982	0.127	0.982
50(40)	A[21]	0.564	0.960	0.698	0.954	0.136	0.982	0.129	0.982	0.124	0.982	0.116	0.983
	B[22]	0.626	0.957	0.754	0.951	0.139	0.981	0.133	0.982	0.125	0.982	0.120	0.982
	C[23]	0.545	0.961	0.680	0.955	0.133	0.982	0.129	0.982	0.124	0.982	0.116	0.983
80(30)	A[11]	0.513	0.963	0.645	0.956	0.129	0.982	0.121	0.982	0.118	0.982	0.114	0.983
	B[12]	0.517	0.963	0.676	0.955	0.131	0.982	0.124	0.982	0.122	0.982	0.115	0.983
	C[13]	0.513	0.963	0.644	0.956	0.128	0.982	0.115	0.983	0.114	0.983	0.112	0.983
80(60)	A[21]	0.421	0.967	0.513	0.963	0.124	0.982	0.112	0.983	0.108	0.983	0.107	0.983
	B[22]	0.447	0.966	0.554	0.961	0.125	0.982	0.114	0.983	0.112	0.983	0.107	0.983
	C[23]	0.404	0.968	0.511	0.963	0.121	0.982	0.111	0.983	0.108	0.983	0.106	0.983

Table 7. The AIL (first col.) and CP (second col.) estimation results of $R(x)$.

$n(k)$	Design	NA-ACI		NT-ACI		BCI				HPD			
						PA		PB		PA		PB	
For Pop-1 $((t_{min}, t_{max}) = (0.2, 0.5))$													
20(10)	A[11]	1.395	0.913	0.586	0.957	0.184	0.979	0.139	0.981	0.084	0.984	0.059	0.985
	B[12]	1.414	0.912	0.674	0.952	0.187	0.979	0.150	0.981	0.089	0.984	0.062	0.985
	C[13]	1.566	0.904	0.740	0.949	0.225	0.977	0.163	0.980	0.097	0.984	0.070	0.985
20(15)	A[21]	1.004	0.934	0.461	0.964	0.109	0.983	0.069	0.985	0.067	0.985	0.054	0.986
	B[22]	1.016	0.934	0.521	0.961	0.122	0.982	0.084	0.984	0.081	0.985	0.058	0.986
	C[23]	1.109	0.929	0.585	0.957	0.135	0.982	0.093	0.984	0.084	0.984	0.059	0.986
50(20)	A[11]	0.835	0.944	0.373	0.969	0.089	0.984	0.048	0.986	0.048	0.986	0.047	0.986
	B[12]	0.863	0.942	0.424	0.966	0.089	0.984	0.049	0.986	0.048	0.986	0.048	0.986
	C[13]	0.970	0.936	0.434	0.965	0.096	0.984	0.065	0.985	0.049	0.986	0.048	0.986
50(40)	A[21]	0.685	0.952	0.194	0.978	0.073	0.985	0.046	0.986	0.041	0.987	0.037	0.987
	B[22]	0.721	0.950	0.262	0.975	0.074	0.985	0.046	0.986	0.044	0.987	0.037	0.987
	C[23]	0.774	0.947	0.305	0.972	0.076	0.985	0.047	0.986	0.045	0.987	0.037	0.987
80(30)	A[11]	0.417	0.966	0.102	0.983	0.060	0.986	0.036	0.987	0.035	0.987	0.027	0.987
	B[12]	0.430	0.966	0.186	0.979	0.063	0.986	0.038	0.987	0.036	0.987	0.028	0.987
	C[13]	0.504	0.962	0.188	0.979	0.063	0.985	0.039	0.987	0.037	0.987	0.032	0.987
80(60)	A[21]	0.293	0.973	0.055	0.986	0.034	0.987	0.027	0.987	0.024	0.988	0.019	0.988
	B[22]	0.323	0.971	0.058	0.986	0.052	0.986	0.034	0.987	0.030	0.987	0.019	0.988
	C[23]	0.392	0.968	0.060	0.986	0.055	0.986	0.035	0.987	0.031	0.987	0.027	0.987
For Pop-1 $((t_{min}, t_{max}) = (0.5, 0.8))$													
20(10)	A[11]	1.392	0.913	0.586	0.957	0.181	0.979	0.136	0.982	0.082	0.985	0.058	0.986
	B[12]	1.411	0.912	0.674	0.952	0.184	0.979	0.147	0.981	0.087	0.984	0.061	0.986
	C[13]	1.564	0.904	0.740	0.949	0.222	0.977	0.160	0.980	0.095	0.984	0.069	0.985
20(15)	A[21]	1.003	0.935	0.461	0.964	0.102	0.983	0.068	0.985	0.066	0.985	0.054	0.986
	B[22]	1.015	0.934	0.521	0.961	0.114	0.983	0.084	0.984	0.079	0.985	0.057	0.986
	C[23]	1.108	0.929	0.584	0.957	0.126	0.982	0.088	0.984	0.082	0.985	0.058	0.986
50(20)	A[11]	0.835	0.944	0.373	0.969	0.085	0.984	0.048	0.986	0.048	0.986	0.046	0.986
	B[12]	0.863	0.942	0.424	0.966	0.086	0.984	0.049	0.986	0.048	0.986	0.047	0.986
	C[13]	0.970	0.936	0.433	0.965	0.092	0.984	0.063	0.986	0.049	0.986	0.048	0.986
50(40)	A[21]	0.685	0.952	0.194	0.978	0.072	0.985	0.043	0.987	0.039	0.987	0.037	0.987
	B[22]	0.721	0.950	0.262	0.975	0.073	0.985	0.044	0.987	0.041	0.987	0.037	0.987
	C[23]	0.773	0.947	0.305	0.972	0.075	0.985	0.047	0.986	0.045	0.987	0.037	0.987
80(30)	A[11]	0.417	0.966	0.102	0.983	0.057	0.986	0.036	0.987	0.035	0.987	0.027	0.987
	B[12]	0.430	0.966	0.186	0.979	0.058	0.986	0.037	0.987	0.036	0.987	0.028	0.987
	C[13]	0.504	0.962	0.188	0.979	0.059	0.986	0.037	0.987	0.037	0.987	0.031	0.987
80(60)	A[21]	0.293	0.973	0.052	0.986	0.033	0.987	0.026	0.988	0.024	0.988	0.017	0.988
	B[22]	0.323	0.971	0.055	0.986	0.052	0.986	0.034	0.987	0.028	0.987	0.018	0.988
	C[23]	0.392	0.968	0.056	0.986	0.055	0.986	0.035	0.987	0.030	0.987	0.027	0.988
For Pop-2 $((t_{min}, t_{max}) = (0.2, 0.5))$													
20(10)	A[11]	1.410	0.913	0.571	0.957	0.078	0.982	0.058	0.983	0.046	0.984	0.045	0.984
	B[12]	1.684	0.898	0.633	0.953	0.081	0.982	0.060	0.983	0.046	0.984	0.045	0.984
	C[13]	1.693	0.898	0.659	0.952	0.083	0.982	0.060	0.983	0.046	0.984	0.046	0.984
20(15)	A[21]	1.040	0.932	0.411	0.965	0.057	0.983	0.044	0.984	0.043	0.984	0.043	0.984
	B[22]	1.248	0.921	0.463	0.962	0.059	0.983	0.044	0.984	0.044	0.984	0.043	0.984
	C[23]	1.299	0.919	0.470	0.962	0.060	0.983	0.045	0.984	0.045	0.984	0.044	0.984
50(20)	A[11]	0.942	0.937	0.359	0.968	0.048	0.984	0.042	0.984	0.042	0.984	0.040	0.984
	B[12]	0.994	0.934	0.367	0.967	0.048	0.984	0.044	0.984	0.042	0.984	0.041	0.984
	C[13]	1.024	0.933	0.385	0.966	0.052	0.984	0.044	0.984	0.042	0.984	0.041	0.984
50(40)	A[21]	0.692	0.950	0.267	0.972	0.045	0.984	0.042	0.984	0.038	0.984	0.036	0.985
	B[22]	0.713	0.949	0.347	0.968	0.046	0.984	0.042	0.984	0.039	0.984	0.036	0.985
	C[23]	0.814	0.944	0.352	0.968	0.047	0.984	0.042	0.984	0.040	0.984	0.037	0.984
80(30)	A[11]	0.394	0.966	0.136	0.979	0.044	0.984	0.039	0.984	0.034	0.985	0.033	0.985
	B[12]	0.554	0.957	0.151	0.978	0.044	0.984	0.041	0.984	0.035	0.985	0.033	0.985
	C[13]	0.581	0.956	0.181	0.977	0.044	0.984	0.041	0.984	0.036	0.985	0.033	0.985
80(60)	A[21]	0.163	0.978	0.081	0.982	0.039	0.984	0.037	0.984	0.028	0.985	0.027	0.985
	B[22]	0.283	0.972	0.101	0.981	0.042	0.984	0.038	0.984	0.029	0.985	0.027	0.985
	C[23]	0.304	0.971	0.131	0.980	0.043	0.984	0.039	0.984	0.034	0.985	0.029	0.985
For Pop-2 $((t_{min}, t_{max}) = (0.5, 0.8))$													
20(10)	A[11]	1.408	0.913	0.571	0.957	0.076	0.982	0.056	0.983	0.046	0.984	0.044	0.984
	B[12]	1.680	0.899	0.633	0.953	0.078	0.982	0.058	0.983	0.046	0.984	0.045	0.984
	C[13]	1.689	0.898	0.658	0.952	0.080	0.982	0.058	0.983	0.046	0.984	0.045	0.984
20(15)	A[21]	1.039	0.932	0.411	0.965	0.056	0.983	0.044	0.984	0.043	0.984	0.042	0.984
	B[22]	1.246	0.921	0.463	0.962	0.058	0.983	0.044	0.984	0.044	0.984	0.043	0.984
	C[23]	1.298	0.919	0.470	0.962	0.058	0.983	0.045	0.984	0.044	0.984	0.044	0.984
50(20)	A[11]	0.942	0.937	0.359	0.968	0.047	0.984	0.042	0.984	0.042	0.984	0.040	0.984
	B[12]	0.993	0.935	0.367	0.967	0.047	0.984	0.043	0.984	0.042	0.984	0.041	0.984
	C[13]	1.023	0.933	0.385	0.966	0.051	0.984	0.043	0.984	0.042	0.984	0.041	0.984
50(40)	A[21]	0.691	0.950	0.267	0.972	0.044	0.984	0.041	0.984	0.038	0.984	0.036	0.985
	B[22]	0.713	0.949	0.347	0.968	0.045	0.984	0.041	0.984	0.039	0.984	0.036	0.985
	C[23]	0.813	0.944	0.352	0.968	0.047	0.984	0.041	0.984	0.039	0.984	0.037	0.984
80(30)	A[11]	0.394	0.966	0.136	0.979	0.042	0.984	0.039	0.984	0.034	0.985	0.033	0.985
	B[12]	0.554	0.957	0.151	0.978	0.043	0.984	0.041	0.984	0.035	0.985	0.033	0.985
	C[13]	0.581	0.956	0.181	0.977	0.043	0.984	0.041	0.984	0.036	0.985	0.033	0.985
80(60)	A[21]	0.163	0.978	0.081	0.982	0.038	0.984	0.037	0.984	0.028	0.985	0.027	0.985
	B[22]	0.283	0.972	0.101	0.981	0.041	0.984	0.038	0.984	0.029	0.985	0.027	0.985
	C[23]	0.304	0.971	0.131	0.980	0.042	0.984	0.038	0.984	0.033	0.985	0.028	0.985

Table 8. The AIL (first col.) and CP (second col.) estimation results of $h(x)$.

$n(k)$	Design	NA-ACI		NT-ACI		BCI				HPD			
						PA		PB		PA		PB	
For Pop-1 $((t_{min}, t_{max}) = (0.2, 0.5))$													
20(10)	A[11]	1.477	0.904	1.856	0.883	0.920	0.936	0.717	0.947	0.477	0.961	0.357	0.968
	B[12]	1.390	0.909	1.764	0.888	0.787	0.943	0.629	0.952	0.422	0.964	0.316	0.970
	C[13]	1.426	0.907	1.803	0.886	0.797	0.943	0.668	0.950	0.435	0.963	0.332	0.969
20(15)	A[21]	1.298	0.914	1.612	0.897	0.573	0.955	0.423	0.964	0.407	0.965	0.308	0.970
	B[22]	1.232	0.918	1.594	0.898	0.522	0.958	0.366	0.967	0.354	0.968	0.298	0.971
	C[23]	1.321	0.913	1.672	0.893	0.624	0.952	0.461	0.962	0.412	0.964	0.312	0.970
50(20)	A[11]	1.175	0.921	1.569	0.899	0.474	0.961	0.344	0.968	0.285	0.972	0.275	0.972
	B[12]	1.045	0.929	1.504	0.903	0.446	0.963	0.280	0.972	0.275	0.972	0.270	0.972
	C[13]	1.165	0.922	1.548	0.900	0.447	0.962	0.283	0.972	0.276	0.972	0.271	0.972
50(40)	A[21]	0.859	0.939	1.336	0.912	0.391	0.966	0.263	0.973	0.254	0.973	0.225	0.975
	B[22]	0.723	0.947	1.319	0.913	0.387	0.966	0.261	0.973	0.246	0.974	0.224	0.975
	C[23]	0.870	0.939	1.446	0.906	0.398	0.965	0.275	0.972	0.263	0.973	0.227	0.975
80(30)	A[11]	0.683	0.949	1.284	0.915	0.353	0.968	0.235	0.974	0.222	0.975	0.197	0.977
	B[12]	0.573	0.955	1.022	0.930	0.337	0.969	0.219	0.975	0.207	0.976	0.177	0.978
	C[13]	0.607	0.953	1.155	0.923	0.350	0.968	0.224	0.975	0.219	0.975	0.183	0.977
80(60)	A[21]	0.387	0.966	0.755	0.945	0.325	0.969	0.209	0.976	0.182	0.977	0.127	0.981
	B[22]	0.336	0.969	0.513	0.959	0.237	0.974	0.204	0.976	0.168	0.978	0.125	0.981
	C[23]	0.466	0.961	0.836	0.941	0.334	0.969	0.212	0.976	0.184	0.977	0.171	0.978
For Pop-1 $((t_{min}, t_{max}) = (0.5, 0.8))$													
20(10)	A[11]	1.247	0.917	1.697	0.892	0.903	0.937	0.701	0.948	0.468	0.961	0.352	0.968
	B[12]	1.131	0.924	1.589	0.898	0.770	0.944	0.614	0.953	0.409	0.965	0.309	0.970
	C[13]	1.195	0.920	1.622	0.896	0.781	0.944	0.653	0.951	0.427	0.964	0.322	0.969
20(15)	A[21]	1.019	0.930	1.496	0.903	0.548	0.957	0.412	0.964	0.406	0.965	0.304	0.971
	B[22]	1.010	0.931	1.469	0.905	0.499	0.960	0.359	0.967	0.349	0.968	0.293	0.971
	C[23]	1.058	0.928	1.525	0.902	0.595	0.954	0.442	0.963	0.406	0.965	0.308	0.970
50(20)	A[11]	0.972	0.933	1.455	0.906	0.459	0.962	0.333	0.969	0.282	0.972	0.272	0.972
	B[12]	0.888	0.938	1.399	0.909	0.431	0.963	0.276	0.972	0.272	0.972	0.267	0.973
	C[13]	0.936	0.935	1.413	0.908	0.432	0.963	0.278	0.972	0.275	0.972	0.271	0.972
50(40)	A[21]	0.783	0.944	1.313	0.914	0.387	0.966	0.258	0.973	0.244	0.974	0.224	0.975
	B[22]	0.647	0.951	1.239	0.918	0.384	0.966	0.250	0.974	0.233	0.975	0.224	0.976
	C[23]	0.793	0.943	1.346	0.912	0.393	0.965	0.266	0.973	0.256	0.973	0.227	0.975
80(30)	A[11]	0.524	0.958	1.154	0.923	0.334	0.969	0.224	0.975	0.222	0.975	0.190	0.977
	B[12]	0.421	0.964	0.865	0.939	0.322	0.970	0.218	0.975	0.204	0.976	0.176	0.978
	C[13]	0.458	0.962	1.061	0.928	0.331	0.969	0.220	0.975	0.219	0.975	0.182	0.977
80(60)	A[21]	0.318	0.970	0.680	0.950	0.312	0.970	0.207	0.976	0.176	0.978	0.121	0.981
	B[22]	0.267	0.973	0.444	0.963	0.206	0.976	0.178	0.978	0.163	0.978	0.118	0.981
	C[23]	0.390	0.966	0.686	0.949	0.319	0.970	0.210	0.976	0.182	0.977	0.171	0.978
For Pop-2 $((t_{min}, t_{max}) = (0.2, 0.5))$													
20(10)	A[11]	1.282	0.921	1.771	0.896	0.200	0.978	0.152	0.980	0.124	0.982	0.123	0.982
	B[12]	1.111	0.930	1.534	0.908	0.192	0.978	0.147	0.980	0.124	0.982	0.119	0.982
	C[13]	1.150	0.928	1.588	0.906	0.196	0.978	0.152	0.980	0.124	0.982	0.121	0.982
20(15)	A[21]	0.815	0.946	1.126	0.930	0.150	0.980	0.119	0.982	0.118	0.982	0.116	0.982
	B[22]	0.724	0.950	0.999	0.936	0.145	0.980	0.119	0.982	0.117	0.982	0.114	0.982
	C[23]	0.874	0.943	1.207	0.925	0.151	0.980	0.120	0.982	0.118	0.982	0.118	0.982
50(20)	A[11]	0.653	0.954	0.902	0.941	0.133	0.981	0.118	0.982	0.117	0.982	0.114	0.982
	B[12]	0.589	0.957	0.813	0.946	0.128	0.981	0.117	0.982	0.116	0.982	0.111	0.982
	C[13]	0.592	0.957	0.817	0.946	0.129	0.981	0.118	0.982	0.116	0.982	0.112	0.982
50(40)	A[21]	0.535	0.960	0.739	0.950	0.123	0.982	0.115	0.982	0.105	0.983	0.103	0.983
	B[22]	0.527	0.961	0.727	0.950	0.122	0.982	0.111	0.982	0.103	0.983	0.102	0.983
	C[23]	0.550	0.959	0.759	0.949	0.125	0.982	0.115	0.982	0.105	0.983	0.105	0.983
80(30)	A[11]	0.472	0.963	0.652	0.954	0.119	0.982	0.107	0.982	0.102	0.983	0.090	0.983
	B[12]	0.449	0.965	0.620	0.956	0.118	0.982	0.106	0.983	0.096	0.983	0.090	0.983
	C[13]	0.463	0.964	0.640	0.955	0.119	0.982	0.107	0.982	0.099	0.983	0.090	0.983
80(60)	A[21]	0.426	0.966	0.588	0.957	0.113	0.982	0.104	0.983	0.082	0.984	0.080	0.984
	B[22]	0.342	0.970	0.473	0.963	0.106	0.983	0.102	0.983	0.080	0.984	0.078	0.984
	C[23]	0.434	0.965	0.600	0.957	0.115	0.982	0.104	0.983	0.094	0.983	0.085	0.984
For Pop-2 $((t_{min}, t_{max}) = (0.5, 0.8))$													
20(10)	A[11]	1.127	0.929	1.488	0.911	0.193	0.978	0.146	0.980	0.124	0.982	0.122	0.982
	B[12]	0.976	0.937	1.289	0.921	0.185	0.978	0.142	0.981	0.123	0.982	0.117	0.982
	C[13]	1.010	0.936	1.334	0.919	0.189	0.978	0.146	0.980	0.124	0.982	0.121	0.982
20(15)	A[21]	0.716	0.951	0.945	0.939	0.148	0.980	0.119	0.982	0.118	0.982	0.113	0.982
	B[22]	0.636	0.955	0.840	0.944	0.142	0.981	0.118	0.982	0.116	0.982	0.113	0.982
	C[23]	0.768	0.948	1.014	0.935	0.148	0.980	0.119	0.982	0.118	0.982	0.114	0.982
50(20)	A[11]	0.574	0.958	0.758	0.949	0.130	0.981	0.118	0.982	0.116	0.982	0.112	0.982
	B[12]	0.518	0.961	0.683	0.953	0.125	0.982	0.116	0.982	0.112	0.982	0.110	0.982
	C[13]	0.520	0.961	0.687	0.952	0.126	0.981	0.117	0.982	0.114	0.982	0.111	0.982
50(40)	A[21]	0.470	0.964	0.621	0.956	0.121	0.982	0.112	0.982	0.104	0.983	0.103	0.983
	B[22]	0.463	0.964	0.611	0.956	0.118	0.982	0.110	0.982	0.103	0.983	0.102	0.983
	C[23]	0.483	0.963	0.638	0.955	0.123	0.982	0.112	0.982	0.105	0.983	0.104	0.983
80(30)	A[11]	0.415	0.966	0.548	0.960	0.117	0.982	0.106	0.983	0.102	0.983	0.090	0.983
	B[12]	0.395	0.968	0.521	0.961	0.115	0.982	0.105	0.983	0.095	0.983	0.089	0.983
	C[13]	0.407	0.967	0.537	0.960	0.116	0.982	0.106	0.983	0.098	0.983	0.090	0.983
80(60)	A[21]	0.374	0.969	0.494	0.962	0.112	0.982	0.103	0.983	0.082	0.984	0.079	0.984
	B[22]	0.301	0.972	0.397	0.967	0.105	0.983	0.100	0.983	0.080	0.984	0.077	0.984
	C[23]	0.382	0.968	0.504	0.962	0.114	0.982	0.103	0.983	0.092	0.983	0.082	0.984

5. Real-World Applications

To demonstrate the practical relevance of the proposed estimation procedures and to illustrate their adaptability to real-world analytical contexts, this section presents two empirical applications from infectious diseases and petroleum engineering. The first application analyzes the timing of infections in dialysis patients, while the second examines shallow permeability measurements expressed in millidarcies.

Next, before reporting the real datasets proposed in Table 9, we present a brief discussion of the datasets that were examined:

- Nephrology Application: Kidney dialysis patients are highly susceptible to infections that can develop and persist over the course of months, largely due to their weakened immune systems and the repeated need for invasive treatment procedures. The use of vascular access devices, including catheters and arteriovenous fistulas, creates potential pathways for microbial entry, increasing the risk of bloodstream and localized infections. Over successive months of treatment, this risk may accumulate, particularly in the presence of comorbid conditions or inadequate infection control measures. In this application, we will study the time intervals of infection in dialysis patients in months. The dataset was reported by Klein and Moeschberger [18] and reanalyzed by Bantan et al. [19].
- Engineering Application: The permeability of a medium reflects its capacity to transmit fluids. These measurements are important in petroleum engineering for characterizing near-surface formations, where variations in permeability can significantly influence fluid flow and reservoir performance. Focusing on shallow permeability provides a more detailed understanding of the heterogeneity and structural properties of the upper layers, which are often most affected by environmental and geological factors. Motivated by this, the present study analyzes permeability measurements (in millidarcies), considering only shallow values. This dataset was originally provided by Ricciardi et al. [20].

Table 9. Data points of hemodialysis and surface permeability.

Data-1: Times of infection in dialysis patients									
0.083	0.083	0.117	0.117	0.117	0.150	0.183	0.217	0.217	0.250
0.250	0.250	0.250	0.283	0.317	0.350	0.383	0.417	0.417	0.450
0.483	0.483	0.717	0.717	0.750	0.750	0.850	0.917		
Data-2: Shallow permeability results									
0.191	0.203	0.214	0.217	0.241	0.248	0.251	0.282	0.292	0.294
0.299	0.305	0.320	0.346	0.353	0.370	0.370	0.370	0.377	0.390
0.402	0.403	0.424	0.425	0.426	0.439	0.447	0.466	0.477	0.484
0.497	0.498	0.523	0.530	0.539	0.558	0.565	0.568	0.585	0.615
0.625	0.640	0.650	0.660	0.680	0.696	0.707	0.799	0.810	0.824
0.832	0.883	0.888	0.937	0.975					

To demonstrate the practical competitiveness of the proposed ULind model, it was compared with eight alternative unit distributions using two biomedical and engineering applications. Notably, five of these competing models have been introduced in the last decade, called the Unit–Weibull, Unit–Gamma, Unit–Gompertz, Unit–log-logistic, and Unit–Birnbaum–Saunders distributions. Hence, the comparative study reflects both classical benchmarks and recent methodological developments in the bounded-distribution literature. Thus, from Data-i for $i = 1, 2$, we will compare its fit with eight competitor models, namely:

(1) Unit–Weibull (UW(θ, ϑ)) by Mazucheli et al. [21];
(2) Unit–gamma (UG(θ, ϑ)) by Mazucheli et al. [22];
(3) Unit–Gompertz (UGom(θ, ϑ)) by Mazucheli et al. [23];
(4) Unit–log–log (ULL(θ, ϑ)) by Korkmaz and Korkmaz [24];
(5) Unit–Birnbaum–Saunders (UBS(θ, ϑ)) by Mazucheli et al. [25];
(6) Topp–Leone (TL(ϑ)) by Topp and Leone [26];
(7) Kumaraswamy (Kum(θ, ϑ)) by Mitnik and Baek [27];
(8) Beta (Beta(θ, ϑ)) by Gupta and Nadarajah [28].

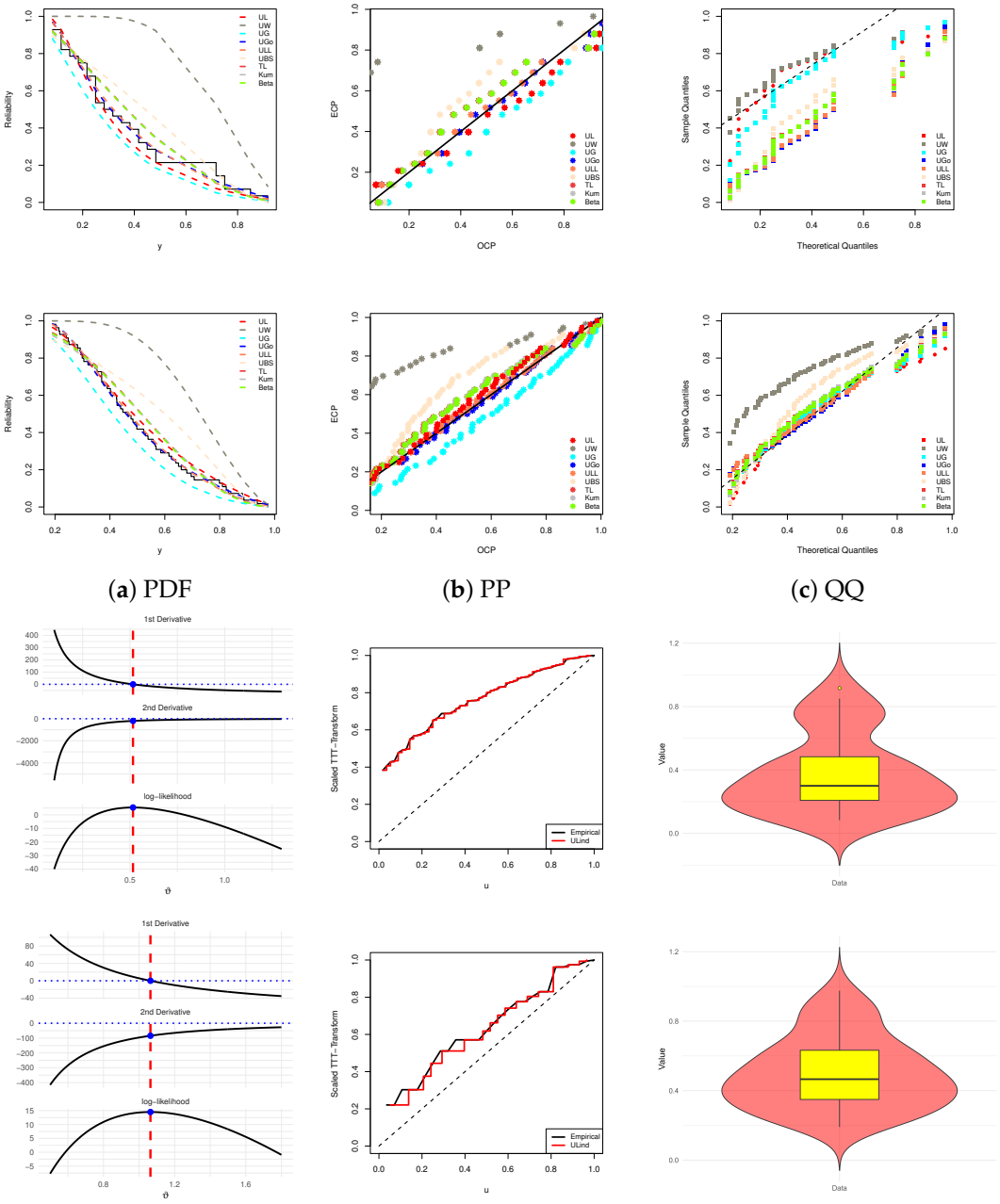
Alongside the Kolmogorov–Smirnov (K-S) statistic and its associated P-value, several model selection metrics are evaluated, including the negative log-likelihood (N-L), Akaike information (A-I), consistent A-I (C-AI), Bayesian information (B-I), Hannan–Quinn information (H-QI), Anderson–Darling (A-D), and Cramér–von Mises (Cv-M); the results are presented in Table 10. These measures are computed using the MLE and its standard error (SE) for θ (or ϑ).

Table 10. Fitting outputs of the ULind and its competitors from Data-i (for $i = 1, 2$).

Model	θ		ϑ		N-L	A-I	C-AI	BI	H-QI	A-D	Cv-M	KS	
	Est.	SE	Est.	SE								Distance	p-Value
Data-1													
ULind	0.0000	0.0000	0.5158	0.0710	−5.3850	−8.7700	−7.4378	−8.6162	−8.3628	0.2942	0.0382	0.1395	0.6468
UW	4.2071	1.1202	1.5704	0.2483	−4.9569	−7.9139	−5.9224	−7.2080	−7.5251	1.8739	0.3316	0.2416	0.1638
UG	2.0681	0.5144	1.7272	0.4859	−4.0047	−4.0095	−1.3450	−3.5295	−3.1949	0.3779	0.0526	0.1818	0.3130
UGom	0.3045	0.2004	1.0093	0.2882	−5.3293	−8.6586	−5.9942	−8.1786	−7.8441	0.2960	0.0400	0.1500	0.6435
ULL	1.3200	0.2168	1.5550	0.1307	−5.2783	−8.5566	−5.8922	−8.0766	−7.7421	0.2972	0.0412	0.1591	0.6405
UBS	0.9316	0.1246	0.8174	0.1290	−0.3916	3.2169	5.8813	3.6969	4.0314	1.2873	0.2257	0.2356	0.0893
TL	0.0000	0.0000	1.3779	0.2604	−3.8524	−5.7049	−4.3727	−5.5510	−5.2976	0.6679	0.1067	0.1442	0.6056
Kum	1.2651	0.2544	2.0797	0.5714	−3.6625	−3.3250	−0.6606	−2.8450	−2.5104	0.7049	0.1136	0.1477	0.6029
Beta	1.3568	0.3332	2.1058	0.5497	−3.7776	−3.5552	−0.8908	−3.0752	−2.7407	0.6859	0.1101	0.1412	0.6321
Data-2													
ULind	0.0000	0.0000	1.0638	0.1089	−14.501	−27.002	−24.994	−26.926	−26.225	0.1301	0.0152	0.0736	0.9268
UW	4.2071	1.1202	1.5704	0.2483	−10.957	−17.914	−15.922	−17.208	−17.525	1.8739	0.3316	0.2416	0.1638
UG	2.2755	0.4062	2.9062	0.5801	−10.063	−16.126	−12.111	−15.895	−14.573	0.3104	0.0418	0.1521	0.1567
UGom	0.2365	0.1085	1.7581	0.3244	−14.482	−26.998	−22.994	−26.778	−25.456	0.1329	0.0165	0.0753	0.9250
ULL	1.4067	0.1631	2.1882	0.1576	−14.280	−26.561	−22.546	−26.330	−25.008	0.1319	0.0164	0.0770	0.9240
UBS	0.9817	0.0938	0.5107	0.0601	3.0551	10.110	14.125	10.341	11.663	2.7879	0.4771	0.2323	0.0053
TL	0.0000	0.0000	2.5878	0.3489	−10.525	−19.050	−17.042	−18.974	−18.273	0.8110	0.1240	0.1101	0.5174
Kum	2.0217	0.2821	2.2792	0.4512	−9.1593	−14.319	−10.304	−14.088	−12.766	1.0376	0.1623	0.1100	0.5192
Beta	2.4026	0.4395	2.2966	0.4182	−9.8130	−15.626	−11.611	−15.395	−14.073	0.9390	0.1457	0.1064	0.5619

To assess the suitability of competing distributions for the observed lifetime datasets, the AdequacyModel package in R (Marinho et al. [29]) is utilized, offering a comprehensive approach for goodness-of-fit evaluation through both numerical and graphical methods. As seen in Table 10, the ULind distribution consistently attains the most favorable values across all criteria, indicating superior model performance. Accordingly, for Data-i, $i = 1, 2$, the ULind lifetime model outperforms alternative distributions.

Graphical diagnostics further support these findings, as illustrated in Figure 5. The plots include: (i) estimated versus fitted reliability curves, (ii) probability–probability (PP) plots, (iii) quantile–quantile (QQ) plots, (iv) scaled total time on test (TTT) transform curves, (v) the log-likelihood profile with respect to the fitted first and second derivatives, and (vi) boxplots overlaid on violin plots. For Data-i (for $i = 1, 2$), Figures 5a–c show that the ULind model provides a satisfactory fit, in agreement with the numerical criteria. The log-likelihood profile in Figure 5d confirms the existence and uniqueness of the MLE $\widehat{\vartheta}$, suggesting it as a reliable initial estimate for further analysis. The TTT curve in Figure 5e indicates an increasing hazard rate, while the distributional visualization in Figure 5f reveals that Data-2 is roughly symmetric, with Data-1 concentrated near the median, though a minor right-skew remains evident.



(**a**) PDF (**b**) PP (**c**) QQ

(**d**) Existence (**e**) TTT (**f**) Violin

Figure 5. Fitting diagrams of the ULind and its competitors from Data-1 (**top**) and Data-2 (**bottom**).

It is worth mentioning here that the empirical TTT plots in Figure 5e exhibit curvature patterns that deviate from the diagonal line, indicating that the underlying HRFs are unlikely to be purely monotone. Instead, these shapes suggest changing risk behavior over time, which may correspond to bathtub-shaped or unimodal hazard structures. Such empirical evidence is broadly consistent with the theoretical flexibility of the ULind model, whose HRF can accommodate increasing, unimodal, and bathtub-shaped forms depending on the parameter value. According to the two case studies proposed, the biomedical data may reflect elevated early risk due to treatment adaptation or patient heterogeneity, followed by stabilization and a later increase caused by disease progression or cumulative complications. Likewise, the engineering data may experience early failures from latent defects or installation problems, followed by a useful-life period and then increasing failure

risk due to aging, fatigue, corrosion, or wear-out effects. Therefore, the ULind model provides an appropriate and flexible framework for modeling both applications.

For each dataset, Data-i ($i = 1, 2$), three artificial I-AP-CT2 samples are generated by fixing $k = 10$ and varying the configurations of S along with the threshold pair (t_{min}, t_{max}), as reported in Table 11. Owing to the absence of prior information on the ULind(ϑ) model derived from Data-i, an improper gamma prior with hyperparameters $a = b = 0.001$ is assumed for Bayesian updating of ϑ. The Bayesian MCMC-based method is initialized at the corresponding MLE of ϑ. From a total of $\nabla = 50{,}000$ iterations, the initial $\nabla^{\circ} = 10{,}000$ samples are discarded as burn-in. The remaining draws are then used to compute Bayesian point estimates and credible intervals for ϑ, the RF $R(x)$, and HRF $h(x)$.

For each sampling scheme $\mathbb{S}[ij]$ for $i = 1, 2$ and $j = 1, 2, 3$, Table 12 summarizes the point estimates with their associated SEs, as well as the corresponding 95% interval estimates and their lengths (ILs), for ϑ, $R(x)$, and $h(x)$. At $x = 0.1$ and 0.2, for Data-i, $i = 1, 2$), respectively, all calculations of $R(x)$ and $h(x)$ are evaluated. The results indicate that both likelihood-based and Bayesian approaches produce closely aligned estimates for all quantities of interest. However, the Bayesian method tends to yield smaller standard errors, and its 95% BCI/HPD intervals are consistently shorter than the analogous 95% NA-ACI/NT-ACI intervals, suggesting a gain in estimation efficiency and precision.

Table 11. Different I-AP-CT2 samples from Data-i (for $i = 1, 2$).

Sample	S	t_{min} (d_{min})	t_{max} (d_{max})	S*	t*	Data
Data-1						
$\mathbb{S}[11]$	$(2^7, 0^7)$	0.85 (14)	0.95 (14)	0	0.75	0.083, 0.117, 0.150, 0.183, 0.217, 0.250, 0.250, 0.250, 0.317, 0.350, 0.417, 0.483, 0.717, 0.750
$\mathbb{S}[12]$	$(0^3, 2^7, 0^4)$	0.26 (7)	0.72 (14)	6	0.717	0.083, 0.083, 0.117, 0.117, 0.183, 0.217, 0.250, 0.283, 0.317, 0.350, 0.450, 0.483, 0.483, 0.717
$\mathbb{S}[13]$	$(0^7, 2^7)$	0.29 (10)	0.40 (12)	10	0.4	0.083, 0.083, 0.117, 0.117, 0.117, 0.150, 0.183, 0.217, 0.250, 0.283, 0.317, 0.383
Data-2						
$\mathbb{S}[21]$	$(3^{10}, 0^{15})$	0.82 (25)	0.85 (25)	0	0.81	0.191, 0.214, 0.217, 0.248, 0.251, 0.282, 0.292, 0.320, 0.346, 0.353, 0.377, 0.403, 0.424, 0.426, 0.439, 0.447, 0.466, 0.484, 0.558, 0.565, 0.640, 0.660, 0.680, 0.707, 0.810
$\mathbb{S}[22]$	$(0^7, 3^{10}, 0^8)$	0.45 (14)	0.71 (25)	9	0.707	0.191, 0.203, 0.214, 0.217, 0.241, 0.248, 0.251, 0.282, 0.320, 0.353, 0.370, 0.390, 0.424, 0.447, 0.466, 0.484, 0.498, 0.523, 0.539, 0.558, 0.565, 0.585, 0.615, 0.650, 0.707
$\mathbb{S}[23]$	$(0^{15}, 3^{10})$	0.43 (18)	0.5 (20)	26	0.5	0.191, 0.203, 0.214, 0.217, 0.241, 0.248, 0.251, 0.282, 0.292, 0.294, 0.299, 0.305, 0.320, 0.346, 0.353, 0.370, 0.377, 0.424, 0.439, 0.498

To show the existence and uniqueness of the MLE $\widehat{\vartheta}$ for ϑ, Figure 6 presents the log-likelihood profiles together with the corresponding score functions across all sampling schemes $\mathbb{S}[ij]$ for $i = 1, 2$, $j = 1, 2, 3$, over a grid of ϑ values. In each case, the profile exhibits a single, prominent peak, confirming both the existence and uniqueness of $\widehat{\vartheta}$. These graphical findings are in agreement with the numerical results reported in Table 12, thereby supporting the use of the obtained MLEs as reliable starting values for subsequent Bayesian procedures.

The convergence behavior of the retained 40,000 MCMC chains from $\mathbb{S}[1j]$ for $j = 1, 2, 3$ as a representative case for ϑ, $R(x)$, and $h(x)$ is examined using trace plots and posterior density plots depicted in Figure 7. The posterior mean and the 95% BCI limits are indicated by solid and dashed black lines, respectively. As observed in Figure 7, the 40,000 Markov chains demonstrate adequate mixing and rapid stabilization for all parameters. The posterior distribution of ϑ appears approximately symmetric, whereas $R(x)$ and $h(x)$ exhibit slight negative and positive skewness, respectively. Based on the 40,000 post-burn-in

samples, various posterior summaries are computed for ϑ, $R(x)$, and $h(x)$, including the mean, mode, quartiles $\mathcal{Q}[i]$, $i = 1, 2, 3$, standard deviation (SD), and skewness (Sk.); see Table 13. These numerical summaries are consistent with the estimates reported in Table 12 as well as the graphical diagnostics in Figure 7.

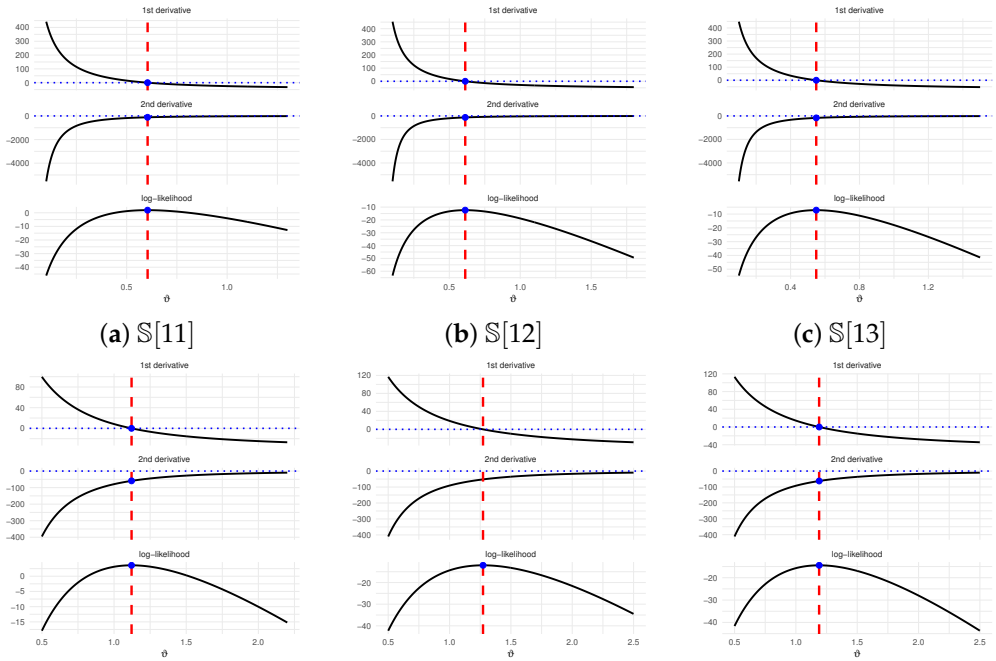
Table 12. Estimates of ϑ, $R(x)$, and $h(x)$ from Data-i (for $i = 1, 2$).

Sample	Par.	MLE MCMC		NA-ACI BCI			NT-ACI HPD		
		Est.	SE	Low.	Upp.	IL	Low.	Upp.	IL
Data-1									
$\mathbb{S}[11]$	ϑ	0.6043	0.0931	0.4219	0.7866	0.3648	0.4468	0.8172	0.3703
		0.6014	0.0563	0.4940	0.7142	0.2202	0.4937	0.7137	0.2200
	$R(x)$	0.9809	0.0146	0.9524	0.9995	0.0471	0.9528	0.9989	0.0461
		0.9784	0.0109	0.9534	0.9923	0.0390	0.9583	0.9944	0.0361
	$h(x)$	1.0085	0.6075	0.0182	2.1991	2.1809	0.3097	3.2839	2.9742
		1.0891	0.4163	0.4847	2.0091	1.5244	0.4165	1.8798	1.4633
$\mathbb{S}[12]$	ϑ	0.6122	0.0890	0.4377	0.7867	0.3491	0.4604	0.8142	0.3538
		0.6094	0.0553	0.5033	0.7204	0.2171	0.5010	0.7176	0.2167
	$R(x)$	0.9821	0.0131	0.9565	1.0078	0.0513	0.9568	0.9947	0.0379
		0.9798	0.0097	0.9567	0.9927	0.0360	0.9611	0.9945	0.0334
	$h(x)$	0.9579	0.5547	0.0293	2.0450	2.0157	0.3079	2.9799	2.6720
		1.0332	0.3783	0.4644	1.8997	1.4353	0.4002	1.7752	1.3750
$\mathbb{S}[13]$	ϑ	0.5489	0.0772	0.3977	0.7002	0.3025	0.4167	0.7230	0.3063
		0.5465	0.0521	0.4468	0.6509	0.2041	0.4462	0.6501	0.2039
	$R(x)$	0.9700	0.0187	0.9333	1.0068	0.0735	0.9340	0.9975	0.0635
		0.9667	0.0210	0.9322	0.9870	0.0548	0.9391	0.9906	0.0515
	$h(x)$	1.4344	0.6921	0.0780	2.7908	2.7128	0.5572	3.6928	3.1356
		1.5246	0.7515	0.7424	2.6544	1.9120	0.6513	2.5087	1.8575
Data-2									
$\mathbb{S}[21]$	ϑ	1.1212	0.1300	0.8664	1.3760	0.5096	0.8933	1.4073	0.5140
		1.1187	0.0619	0.9987	1.2418	0.2431	0.9974	1.2401	0.2427
	$R(x)$	0.9649	0.0170	0.9316	0.9981	0.0665	0.9322	0.9987	0.0665
		0.9636	0.0203	0.9448	0.9776	0.0328	0.9471	0.9791	0.0320
	$h(x)$	0.8659	0.3178	0.2431	1.4887	1.2457	0.4218	1.7777	1.3559
		0.8840	0.1710	0.6123	1.2154	0.6031	0.5904	1.1852	0.5949
$\mathbb{S}[22]$	ϑ	1.2727	0.1385	1.0013	1.5441	0.5429	1.0283	1.5752	0.5470
		1.2701	0.0628	1.1481	1.3943	0.2462	1.1485	1.3945	0.2460
	$R(x)$	0.9801	0.0104	0.9597	1.0004	0.0407	0.9599	0.9992	0.0393
		0.9793	0.0057	0.9682	0.9874	0.0192	0.9697	0.9883	0.0186
	$h(x)$	0.5593	0.2281	0.1122	1.0064	0.8942	0.2515	1.2440	0.9926
		0.5724	0.3997	0.3888	0.8023	0.4135	0.3755	0.7819	0.4063
$\mathbb{S}[23]$	ϑ	1.1895	0.1266	0.9414	1.4376	0.4961	0.9656	1.4653	0.4997
		1.1871	0.0616	1.0679	1.3092	0.2413	1.0674	1.3084	0.2410
	$R(x)$	0.9728	0.0129	0.9475	0.9980	0.0505	0.9478	0.9983	0.0505
		0.9718	0.0122	0.9572	0.9826	0.0254	0.9587	0.9835	0.0248
	$h(x)$	0.7127	0.2598	0.2035	1.2218	1.0183	0.3489	1.4560	1.1072
		0.7279	0.2637	0.5021	1.0053	0.5032	0.4846	0.9811	0.4964

Figure 8 provides a clear comparative view of the four interval estimation methods for both the reliability function $R(x)$ and the hazard rate function $h(x)$ across the three scenarios $S[ij]$ for $i = 1, 2$, $j = 1, 2, 3$. As a result, it can be seen that:

- For $R(x)$, all methods exhibit the expected monotonically decreasing trend. It also indicates that the HPD-based approach yields more precise interval estimates while maintaining stability.
- For $h(x)$, all methods consistently capture the increasing trend, although greater variability is observed compared to $R(x)$, especially for small values of y. As y increases, the intervals narrow and become more stable.

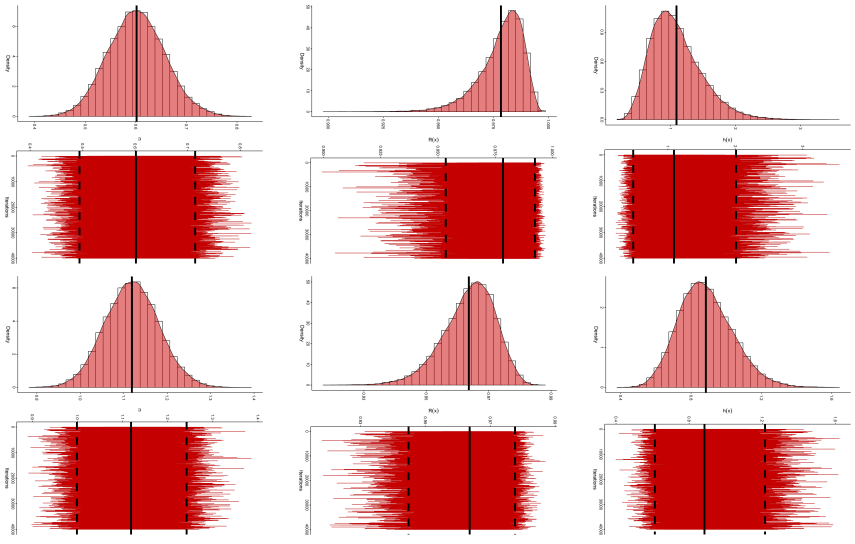
- Overall, the results suggest that while all methods perform reasonably well, the HPD-based intervals offer a more favorable balance between precision and reliability, making them an efficient choice for interval estimation of both $R(x)$ and $h(x)$.
- Additionally, for both $R(x)$ and $h(x)$, the accuracy of the estimated interval bounds becomes tighter at progresses from $S[i1]$ to $S[i3]$ for $i = 1, 2$, suggesting improved estimation accuracy.



(**a**) $\mathbb{S}[11]$ (**b**) $\mathbb{S}[12]$ (**c**) $\mathbb{S}[13]$

(**d**) $\mathbb{S}[21]$ (**e**) $\mathbb{S}[22]$ (**f**) $\mathbb{S}[23]$

Figure 6. Plots of log-likelihood/score functions of ϑ from Data-1 (**top**) and Data-2 (**bottom**).



(**a**) ϑ (**b**) $R(x)$ (**c**) $h(x)$

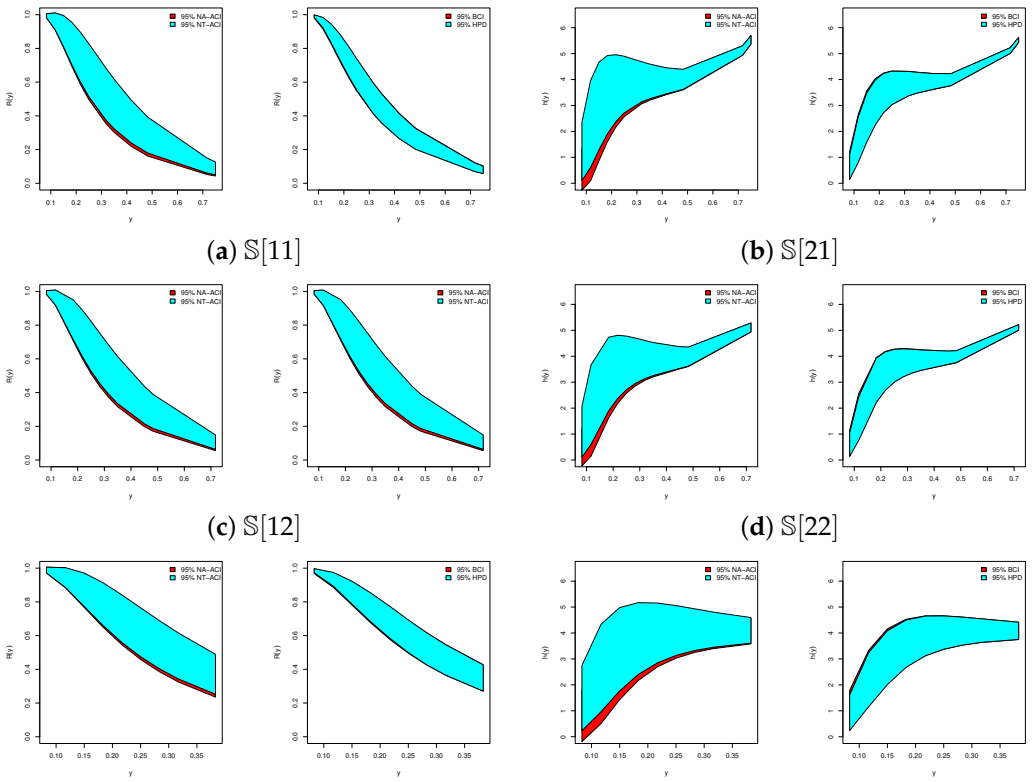
Figure 7. Convergence diagnostics of ϑ, $R(x)$, and $h(x)$ from Data-1 (**top**) and Data-2 (**bottom**).

In summary, the analyses based on samples generated under the proposed censoring scheme, when applied to both the infectious disease and petroleum engineering datasets, provide a thorough assessment of the ULind lifetime model. The empirical findings are in close agreement with the simulation outcomes and further highlight the practical

effectiveness of the proposed methodology for reliability analysis in both biomedical and engineering applications.

Table 13. Statistics of ϑ, $R(x)$, and $h(x)$ from Data-i (for $i = 1, 2$).

Sample	Par.	Mean	Mode	$\mathcal{Q}[1]$	$\mathcal{Q}[2]$	$\mathcal{Q}[3]$	SD	Sk.
Data-1								
$\mathbb{S}[11]$	ϑ	0.6014	0.5699	0.5630	0.6008	0.6390	0.0562	0.0770
	$R(x)$	0.9784	0.9747	0.9733	0.9804	0.9857	0.0102	−1.2999
	$h(x)$	1.0891	1.1054	0.8035	1.0315	1.3132	0.3951	0.8872
$\mathbb{S}[12]$	ϑ	0.6094	0.5779	0.5716	0.6088	0.6464	0.0552	0.0685
	$R(x)$	0.9798	0.9763	0.9751	0.9816	0.9865	0.0094	−1.2838
	$h(x)$	1.0332	0.9885	0.7651	0.9795	1.2431	0.3707	0.8858
$\mathbb{S}[13]$	ϑ	0.5465	0.5146	0.5110	0.5459	0.5814	0.0521	0.0765
	$R(x)$	0.9667	0.9605	0.9593	0.9693	0.9770	0.0143	−1.1672
	$h(x)$	1.5246	1.1637	1.1681	1.4618	1.8121	0.4935	0.7697
Data-2								
$\mathbb{S}[21]$	ϑ	1.1187	1.0869	1.0765	1.1185	1.1606	0.0619	0.0321
	$R(x)$	0.9636	0.9601	0.9585	0.9645	0.9697	0.0084	−0.6397
	$h(x)$	0.8840	0.9535	0.7744	0.8726	0.9816	0.1542	0.4279
$\mathbb{S}[22]$	ϑ	1.2701	1.2258	1.2273	1.2700	1.3124	0.0627	0.0244
	$R(x)$	0.9793	0.9762	0.9764	0.9799	0.9828	0.0049	−0.6726
	$h(x)$	0.5724	0.5774	0.4972	0.5638	0.6388	0.1058	0.4754
$\mathbb{S}[23]$	ϑ	1.1871	1.1552	1.1452	1.1869	1.2287	0.0616	0.0288
	$R(x)$	0.9718	0.9690	0.9679	0.9725	0.9765	0.0065	−0.6459
	$h(x)$	0.7279	0.7864	0.6361	0.7180	0.8091	0.1290	0.4434



(**a**) $\mathbb{S}[11]$ (**b**) $\mathbb{S}[21]$

(**c**) $\mathbb{S}[12]$ (**d**) $\mathbb{S}[22]$

(**e**) $\mathbb{S}[13]$ (**f**) $\mathbb{S}[23]$

Figure 8. Plots for 95% interval limits of $R(x)$ (**left**) and $h(x)$ (**right**) from Data-i (for $i = 1, 2$).

6. Concluding Remarks and Future Research

This study has developed a unified and flexible inferential framework for the ULind model when I-AP-CT2 is available, motivated by the need to analyze bounded lifetime data arising from realistic experimental conditions. By integrating advanced censoring mechanisms with a parsimonious yet highly adaptable probabilistic model, the proposed methodology provides a practical solution for handling incomplete data structures commonly encountered in reliability and survival studies. The combined use of frequentist and Bayesian approaches has enabled a comprehensive assessment of parameter estimation, reliability characteristics, and uncertainty quantification, offering a balanced perspective on both theoretical and applied aspects of inference. From a methodological standpoint, the results confirm that the ULind model is capable of capturing diverse failure behaviors through its flexible hazard rate structure, making it particularly suitable for modeling complex risk patterns observed in practice. The incorporation of the I-AP-CT2 scheme further enhances applicability by ensuring controlled experimental duration while maintaining inferential efficiency. The comparative findings also demonstrate the clear advantages of Bayesian estimation—especially when supported by informative priors—in terms of stability, precision, and interval performance under censoring. Moreover, the analysis of different censoring designs provides useful practical guidance, indicating that the choice of censoring configuration should depend on the specific reliability measure of interest. The real data applications reinforce the practical value of the proposed framework. In the context of kidney dialysis data, the methodology offers meaningful insights into patient survival dynamics and risk progression, which are essential for improving treatment evaluation and clinical decision-making. Similarly, in petroleum engineering applications, the model facilitates accurate assessment of system reliability and failure behavior, contributing to more effective maintenance planning and risk mitigation strategies. These findings highlight the broad applicability of the proposed approach across diverse scientific and industrial domains.

Despite these contributions, several areas remain open for further research and deserve further study:

- Incorporating covariates into the ULind model would allow for the development of regression-based reliability models, enabling the study of explanatory factors influencing failure behavior in medical and engineering applications.
- Future work may explore extensions of the ULind distribution with additional shape parameters or its integration into more flexible families (e.g., generalized or compounded models) to further enhance modeling capability.
- The proposed framework can be extended to other complex censoring schemes, such as accelerate tests, competing risks, or progressively first-failure censoring, to broaden its applicability in diverse experimental settings.
- Investigating robust priors, hierarchical Bayesian structures, or nonparametric Bayesian methods could improve inference in situations with limited or uncertain prior information.
- Developing criteria for selecting optimal censoring schemes under cost, time, and efficiency constraints would provide valuable guidance for practitioners designing life-testing experiments.
- The use of more advanced simulation techniques, such as Hamiltonian Monte Carlo or variational inference, may enhance computational efficiency and scalability for large datasets or complex models.
- Future studies may apply the proposed methodology to other fields involving bounded lifetime data, such as environmental studies, financial risk modeling, and reliability of renewable energy systems.

https://doi.org/10.3390/axioms15050310

In summary, this work not only advances the theoretical development of reliability inference under complex censoring but also provides a practically viable framework for real-world applications. The proposed methodology opens several promising directions for future research, with the potential to further bridge the gap between statistical theory and applied reliability analysis.

Author Contributions: Methodology, H.S.M., A.E., O.E.A.-K. and A.A.-H.; software, A.E.; validation, A.E.; resources, O.E.A.-K.; data curation, A.A.-H.; supervision H.S.M.; writing–original draft, O.E.A.-K. and A.A.-H.; writing–review and editing A.E. and H.S.M.; funding acquisition, H.S.M. All authors have read and agreed to the published version of the manuscript.

Funding: This research was funded by the Princess Nourah bint Abdulrahman University Researchers Supporting Project number (PNURSP2026R175), Princess Nourah bint Abdulrahman University, Riyadh, Saudi Arabia.

Data Availability Statement: The authors confirm that the data supporting the findings of this study are available within the article.

Conflicts of Interest: The authors declare no conflict of interest.

Appendix A. The HRF Shapes of the ULind Model

Theorem A1. *Let X be a random variable with HRF given by Equation (4). Then, the HRF exhibits flexible shapes depending on the parameter ϑ. In particular:*

1. *For small values of ϑ, the HRF has a bathtub shape.*
2. *For moderate values of ϑ, the HRF becomes unimodal.*
3. *For large values of ϑ, the HRF is monotonically increasing.*

Proof. Let

$$\mathcal{Q}(y) = y(1+\vartheta)e^{\vartheta y^{\star}} - (y+\vartheta),$$

so that

$$h(y) = \frac{\vartheta^2}{y^2\mathcal{Q}(y)}.$$

First, we study the limiting behavior.
As $y \to 0^+$, we have $y^{\star} \to \infty$, and hence $e^{\vartheta y^{\star}} \to \infty$. Thus,

$$\mathcal{Q}(y) \sim y(1+\vartheta)\exp(\vartheta/y) \to \infty,$$

which implies

$$\lim_{y\to 0^+} h(y) = 0.$$

Next, as $y \to 1^-$, we obtain $y^{\star} \to 0$ and $\exp(\cdot) \to 1$, so that

$$\mathcal{Q}(y) \to (1+\vartheta) - (1+\vartheta) = 0.$$

Therefore,

$$\lim_{y\to 1^-} h(y) = \infty.$$

Now, we analyze the first derivative of $h(y)$ as follows:

$$h^{\star}(y) = \frac{\mathrm{d}}{\mathrm{d}y}\left(\frac{\vartheta^2}{y^2\mathcal{Q}(y)}\right).$$

After simplification, we obtain

$$h^{\star}(y) = -\frac{1}{y\mathcal{Q}(y)}[2\mathcal{Q}(y) + y\mathcal{Q}^{\star}(y)]h(y),$$

where $\mathcal{Q}^{\star}(y) = (1+\vartheta)\left(1-\frac{\vartheta}{y}\right)e^{\vartheta y^{\star}} - 1$.

Thus, the sign of $h^{\star}(y)$ depends on the function

$$\Psi(y) = 2\mathcal{Q}(y) + y\mathcal{Q}^{\star}(y).$$

As a result, we can summarize the behavior of $h(y)$ as follows:

(i) For small values of ϑ, the exponential term $e^{\vartheta y^{\star}}$ grows slowly, and $\mathcal{Q}(y)$ behaves approximately like a polynomial function. In this case, $\Psi(y)$ changes sign twice, implying that $h(y)$ first increases, then decreases, and finally increases again. Hence, the HRF exhibits a bathtub shape.

(ii) For moderate values of ϑ, the exponential term becomes more influential, reducing the region where $\Psi(y) < 0$. Consequently, $h(y)$ has a single turning point, yielding a unimodal shape.

(iii) For large values of ϑ, the exponential term dominates the behavior of $\mathcal{Q}(y)$, and it can be verified that $\Psi(y) > 0$ for all $y \in (0,1)$. Therefore, $h^{\star}(y) > 0$, and the HRF is monotonically increasing.

This completes the proof. □

References

1. Mazucheli, J.; Bapat, S.R.; Menezes, A.F.B. A new one-parameter unit-Lindley distribution. *Chil. J. Stat.* **2020**, *11*, 53–67.
2. Balakrishnan, N.; Cramer, E. *The Art of Progressive Censoring*; Springer: Berlin/Heidelberg, Germany, 2014.
3. Kundu, D.; Joarder, A. Analysis of Type-II progressively hybrid censored data. *Comput. Stat. Data Anal.* **2006**, *50*, 2509–2528. [CrossRef]
4. Ng, H.K.T.; Kundu, D.; Chan, P.S. Statistical analysis of exponential lifetimes under an adaptive Type-II progressive censoring scheme. *Nav. Res. Logist.* **2009**, *56*, 687–698. [CrossRef]
5. Yan, W.; Li, P.; Yu, Y. Statistical inference for the reliability of Burr-XII distribution under improved adaptive Type-II progressive censoring. *Appl. Math. Model.* **2021**, *95*, 38–52. [CrossRef]
6. Bain, L.J.; Engelhardt, M. *Statistical Analysis of Reliability and Life-Testing Models*, 2nd ed.; Marcel Dekker: New York, NY, USA, 1991.
7. Nassar, M.; Elshahhat, A. Estimation procedures and optimal censoring schemes for an improved adaptive progressively type-II censored Weibull distribution. *J. Appl. Stat.* **2024**, *51*, 1664–1688. [CrossRef] [PubMed]
8. Elshahhat, A.; Alotaibi, R.; Nassar, M. Analysis of Weibull time metrics using normal operating via partially accelerated tests with improved adaptive progressive censoring and its applications. *Sci. Rep.* **2025**, *15*, 39548. [CrossRef]
9. Zhang, L.; Yan, R. Parameter estimation of Chen distribution under improved adaptive type-II progressive censoring. *J. Stat. Comput. Simul.* **2024**, *94*, 2830–2861. [CrossRef]
10. Dey, A.; Kayal, S. Statistical Inference of a Chen Lifetime Competing Risks Model Based on Improved Adaptive Type-II Progressive Censored Data. *Qual. Reliab. Eng. Int.* **2026**, *42*, 185–211. [CrossRef]
11. Henningsen, A.; Toomet, O. maxLik: A package for maximum likelihood estimation in R. *Comput. Stat.* **2011**, *26*, 443–458. [CrossRef]
12. Greene, W.H. *Econometric Analysis*, 4th ed.; Prentice-Hall: New York, NY, USA, 2000.
13. Lawless, J.F. *Statistical Models and Methods for Lifetime Data*, 2nd ed.; John Wiley and Sons: New York, NY, USA, 2011.
14. Meeker, W.Q.; Escobar, L.A. *Statistical Methods for Reliability Data*; John Wiley and Sons: New York, NY, USA, 2014.
15. Gelman, A.; Carlin, J.B.; Stern, H.S.; Rubin, D.B. *Bayesian Data Analysis*, 2nd ed.; Chapman and Hall/CRC: Boca Raton, FL, USA, 2004.
16. Plummer, M.; Best, N.; Cowles, K.; Vines, K. CODA: Convergence diagnosis and output analysis for MCMC. *R News* **2006**, *6*, 7–11.
17. Kundu, D. Bayesian inference and life testing plan for the Weibull distribution in presence of progressive censoring. *Technometrics* **2008**, *50*, 144–154. [CrossRef]
18. Klein, J.P.; Moeschberger, M.L. *Survival Analysis: Techniques for Censored and Truncated Data*; Springer: New York, NY, USA, 2003; Volume 1230.

19. Bantan, R.A.; Chesneau, C.; Jamal, F.; Elgarhy, M.; Tahir, M.H.; Ali, A.; Anam, S. Some new facts about the unit-Rayleigh distribution with applications. *Mathematics* **2020**, *8*, 1954. [CrossRef]
20. Ricciardi, K.L.; Pinder, G.F.; Belitz, K. Comparison of the lognormal and beta distribution functions to describe the uncertainty in permeability. *J. Hydrol.* **2005**, *313*, 248–256. [CrossRef]
21. Mazucheli, J.; Menezes, A.F.B.; Fernandes, L.B.; De Oliveira, R.P.; Ghitany, M.E. The unit-Weibull distribution as an alternative to the Kumaraswamy distribution for the modeling of quantiles conditional on covariates. *J. Appl. Stat.* **2020**, *47*, 954–974. [CrossRef]
22. Mazucheli, J.; Menezes, A.F.B.; Dey, S. Improved maximum-likelihood estimators for the parameters of the unit-gamma distribution. *Commun. Stat.-Theory Methods* **2018**, *47*, 3767–3778. [CrossRef]
23. Mazucheli, J.; Menezes, A.F.; Dey, S. Unit-Gompertz distribution with applications. *Statistica* **2019**, *79*, 25–43.
24. Korkmaz, M.Ç.; Korkmaz, Z.S. The unit log–log distribution: A new unit distribution with alternative quantile regression modeling and educational measurements applications. *J. Appl. Stat.* **2023**, *50*, 889–908. [CrossRef]
25. Mazucheli, J.; Menezes, A.F.; Dey, S. The unit-Birnbaum-Saunders distribution with applications. *Chil. J. Stat.* **2018**, *9*, 47–57.
26. Topp, C.W.; Leone, F.C. A family of J-shaped frequency functions. *J. Am. Stat. Assoc.* **1955**, *50*, 209–219. [CrossRef]
27. Mitnik, P.A.; Baek, S. The Kumaraswamy distribution: Median-dispersion re-parameterizations for regression modeling and simulation-based estimation. *Stat. Pap.* **2013**, *54*, 177–192. [CrossRef]
28. Gupta, A.K.; Nadarajah, S. *Handbook of Beta Distribution and Its Applications*; CRC Press: Boca Raton, FL, USA, 2004.
29. Marinho, P.R.D.; Silva, R.B.; Bourguignon, M.; Cordeiro, G.M.; Nadarajah, S. AdequacyModel: An R package for probability distributions and general purpose optimization. *PLoS ONE* **2019**, *14*, e0221487. [CrossRef] [PubMed]

Disclaimer/Publisher's Note: The statements, opinions and data contained in all publications are solely those of the individual author(s) and contributor(s) and not of MDPI and/or the editor(s). MDPI and/or the editor(s) disclaim responsibility for any injury to people or property resulting from any ideas, methods, instructions or products referred to in the content.